1 General information

1.1 Synthesis

All manipulations of oxygen and moisture-sensitive materials were conducted with a standard Schlenk technique. All glassware was kept in an oven at 80°C. Argon atmosphere was generated by three repetitive cycles of vacuum/Argon using a schlenk ramp. Commercially available reagents and solvents were used without further purification other than those detailed below. THF was obtained through a PURE SOLV™ solvent purification system. Light petroleum refers to the fraction with bp 40-60°C. Analytical thin layer chromatography was carried out using aluminum backed plates coated with Merck Kieselgel 60 GF254 and visualized under UV light (at 254 and 360 nm). Flash chromatography was carried out using Teledyne Isco CombiFlash® Rf 400 (UV detection 200-360nm), over standard silica cartridges (Redisep® Isco or Puriflash® columns Interchim).^{1}H and ^{13}C NMR spectra were recorded using Bruker 300 MHz instruments (^{1}H frequency, corresponding ^{13}C frequency: 75 MHz); chemical shifts were recorded in ppm and J values in Hz. The residual signals for the NMR solvents used are 5.32 ppm (proton) and 54.00 ppm (carbon) for CD2Cl2.[1]. The following abbreviations have been used for the NMR assignment: s for singlet, d for doublet, t for triplet, q for quadruplet and m for multiplet. High resolution mass spectra were recorded at the Centre Régional de Mesures Physiques de l'Ouest (CRMPO-Rennes) on a Thermo Ficher Q-Exactive instrument or a Bruker MaXis 4G or a Bruker Ultraflex III.

1.2 X-ray

Crystals were picked up with a cryoloop and then frozen at 150 K under a stream of dry N_2. Data were collected on a D8 VENTURE Bruker AXS diffractometer with Mo–Kα radiation (λ = 0.71073 Å).

Structures were solved by direct methods (SIR92)[2] and refined (SHELXL-2014/7)[3] by full-matrix least-squares methods as implemented in the WinGX software package.[4] An empirical absorption (multi-scan) correction was applied. Hydrogen atoms were introduced at calculated positions (riding model) included in structure factor calculation but not refined. Refinement parameters are summarized in Table S 11 and Table S 12.

Crystallographic data have been deposited with the Cambridge Crystallographic Data Centre as supplementary publication data: **SPA-DBS** (CCDC 2149596), **SIA-DBS** (CCDC 2149597). Copies of the data can be obtained free of charge on application to CCDC, 12 Union Road, Cambridge CB2 1EZ, UK [fax: (+44) 1223-336-033; e-mail: deposit@ccdc.cam.ac.uk].

Figures were generated with Mercury software 3.9.

1.3 Spectroscopic studies

Cyclohexane (spectroscopic grade, Acros), THF (spectroscopic grade, Acros), dichloromethane (spectroscopic grade, Acros), acetronitrile (spectroscopic grade, Acros), methanol (spectroscopic grade, Acros), 2-MeTHF (spectroscopic grade, sigma aldrich), 1 N solution of sulfuric acid in water (Standard solution, Alfa Aesar), and quinine sulfate dihydrate (99+%, ACROS organics) were used without further purification.

UV - visible spectra were recorded using an UV - Visible spectrophotometer JASCO - V630BIO. Molar extinction coefficients (ε) were calculated from the gradients extracted from the plots of absorbance *vs* concentration with five solutions of different concentrations for each sample and at least two mother solutions were prepared.

$$A = \varepsilon \times l \times C$$

Above, l refers to the path length and C to the sample concentration.

Emission spectra were recorded with a HORIBA Scientific Fluoromax-4 equipped with a Xenon lamp. Singlet energy levels were calculated from the onset of the fluorescence spectrum at RT. Conversion in electron-volt was obtained with the following formula:

$$E(eV) = \frac{hc}{\lambda}$$ with h = 6.62607×10^{-34} J.s, c = 2.99792×1017 nm.s^{-1} and 1 eV = 1.60218×10^{-19} J. This equation can be simplified as: formulated in nm.

$$E(eV) = \frac{1239.84}{\lambda}$$

with λ formulated in nm

Quantum yields in solution ($ø_{sol}$) were calculated relative to quinine sulfate ($ø_{ref}$ = 0.546 in H_2SO_4 1 N). $ø_{sol}$ was determined according to the following equation,

$$\phi sol = \phi ref \times \frac{Grad_s}{Grad_r} \times \left(\frac{\eta_s}{\eta_r}\right)^2$$

where subscripts *s* and *r* refer respectively to the sample and reference, *Grad* is the gradient from the plot of integrated fluorescence intensity *vs* absorbance, η is the refracting index of the solvent (η_s = 1.426 for cyclohexane). Five solutions of different concentration (A < 0.1) of the sample and five solutions of the reference (quinine sulfate) were prepared. The integrated area of the fluorescence peak was plotted against the absorbance at the excitation wavelength for both the sample and reference. The gradients of these plots were then injected in the equation to calculate the reported quantum yield value for the sample.

Lipper-Mataga-Ooshika formalism[5-7] was used to estimate the excited state dipole moment.

$$\Delta\nu = \frac{2(\Delta\mu)^2}{r^3 hc}\Delta f + C \quad \text{with} \quad \Delta f = \left(\frac{\varepsilon - 1}{2\varepsilon + 1} - \frac{n^2 - 1}{n^2 + 1}\right)$$

With Δν (cm^{-1}) being the Stokes shift, Δμ (D) the dipole moment difference between S_0 and S_1 states, r (cm) the radius of the solvation sphere obtained from geometry optimisation at the ground state (DFT b3lyp 6-31g(d)), h the Planck constant (6.626.10-34 m^2 .kg.s^{-1}), c the celerity (2,998x10^8 m.s^{-1}), Δf the orientation polarisability of the solvent calculated from its dielectric constant ε (F.m^{-1}) and its refractive index n, and C a constant.

Experimentally, Δν were calculated from the maximal wavelength in absorption and emission spectra measured in five different solvents (cyclohexane, dichloromethane, tetrahydrofuran,methanol and acetonitrile). Δf were calculated from ε and n for the five different solvents. Then,Δf as a function of Δν was plotted and the slope is calculated using a linear regression. Finally,Δμ is calculated as follow:

$$\Delta\mu = \sqrt{\frac{r^3 hc.slope}{2}}$$

Excited state dipole moment μ* is then calculated from the ground state dipole moment μ

estimated by DFT calculations and Δμ.

Absolute quantum yields of the films were recorded using a deported HORIBA Scientific Quanta-Phi integrating sphere linked to the Fluoromax-4.

Fluorescent decay measurements were carried out on the HORIBA Scientific Fluoromax-4 equipped with its TCSPC pulsed source interface.

Spin-coated films were prepared form a 1g/mL in THF solution using a Labspins Tournette from Süss Microtec.

1.4 Electrochemical studies

Electrochemical experiments were performed under argon atmosphere using a Pt disk electrode (diameter 1 mm). The counter electrode was a vitreous carbon rod. The reference electrode was either a silver wire in a 0.1 M $AgNO_3$ solution in CH_3CN for the studies in oxidation or a Silver wire coated by a thin film of AgI (silver(I)iodide) in a 0.1 M Bu_4NI solution in DMF for the studies in reduction. Ferrocene was added to the electrolyte solution at the end of a series of experiments. The ferrocene/ferrocenium (Fc/Fc^+) couple served as internal standard. The three electrodes cell was connected either to a PAR Model 273 potentiostat/galvanostat (PAR, EG&G, USA) monitored with the ECHEM Software or to a potentiostat/galvanostat (Autolab/PGSTAT101) monitored with the Nova 2.1 Software. Activated Al_2O_3 was added in the electrolytic solution to remove excess moisture. For a further comparison of the electrochemical and optical properties, all potentials are referred to the SCE electrode that was calibrated at - 0.405 V *vs.* Fc/Fc^+ system. Following the work of Jenekhe,[8] we estimated the electron affinity (EA) or lowest unoccupied molecular orbital (LUMO) and the ionization potential (IP) or highest occupied molecular orbital (HOMO) from the redox data. The LUMO level was calculated from: LUMO (eV) = -[E_{onset}^{red} (*vs* SCE) + 4.4]. Similarly the HOMO level was calculated from: HOMO (eV) = -[E_{onset}^{ox} (*vs* SCE) + 4.4], based on a SCE energy level of 4.4 eV relative to the vacuum. The electrochemical gap was calculated from: ΔE^{el} =|HOMO-LUMO (in eV).

1.5 Theoretical modelling

Full geometry optimization of the ground state and vibrational frequency calculation were performed with Density Functional Theory (DFT)[9-10] using the hybrid Becke-3 parameter exchange functional [11-13] and the Lee-Yang-Parr non-local correlation functional[14] (B3LYP) implemented in the Gaussian 16 program suite,[15] using the 6-31G(d) basis set and the default convergence criterion implemented in the program. Geometry optimization was performed starting from the X-ray diffraction crystal structure geometry. All stationary points were characterized as minima by analytical frequency calculations.

Optical transition diagrams were obtained through TD-DFT calculations performed using the B3LYP functionals and the 6-311+G(d,p) basis set from the geometry of S_0.

Calculations were carried out on the OCCIGEN calculator of the Centre Informatique National de l'Enseignement Supérieur (CINES (Montpellier) under project N° 2021-A0100805032).

Figures were generated with GaussView 6.0 and GaussSum 3.0.

1.6 Thermal analysis

Thermal Gravimetric Analysis (TGA) was carried out by using a Mettler-Toledo TGA-DSC-1apparatus. TGA curved were measured at 10° C/min from 30° C to 1000° C under a nitrogen flux. Differential Scanning Calorimetry (DSC) was carried out by using a NETZSCH DSC 200 F3 instrument equipped with an intracooler DSC traces were measured at 10° C/min, 2 heating/cooling cycles were successively carried out under a nitrogen flux.

1.7 Devices fabrication and characterization

Devices were fabricated on patterned ITO glass substrates (activating area 0.1 cm^2; 32 mm × 32 mm × 0.7 mm) with a sheet resistance of 15 Ω per square. Before device fabrication, ITO substrates were cleaned with ethanol, acetone, and deionized water, dried in an oven at 120 ° C for 2 h, then treated with UV-ozone for 20 min, and finally loaded into a deposition chamber with a basic pressure of 4.0 × 10^{-6} Torr. The device structure is ITO/HAT-CN (10 nm)/TAPC (40 nm)/TCTA (10 nm)/mCP: emitters (20 nm, x wt%)/TmPyPB (45 nm)/Liq (2 nm)/Al(120 nm). The evaporation rates and thicknesses of organic layers (2-4 Å s^{-1}) , Liq layer (0.1-0.2 Å s^{-1}), and aluminum cathode (4-8 Å s^{-1}) were monitored with oscillating quartz crystals, respectively. The devices were well encapsulated with glued glass lids before testing. The Electroluminescence spectra and current density-voltage (L-J-V) characteristics of

the devices were measured using a constant current source (Keithley 2400 SourceMeter) combined with a photometer (Photo Research SpectraScan PR 655).

2 Synthetic procedures

Compounds **1** and **2** are commercially available. Compounds **3** and **4** were previously synthesized in other studies. All relevant information for synthetic procedures and characterizations can be found in literature[16-17]

2.1 General procedure

1st step: The halogen derivative (1.0 eq) was dissolved in dry THF under argon and the mixture was cooled to -78°C. *n*-BuLi (1.2 eq) was then added dropwise and the resulting mixture was stirred for 30 min at -78°C. Dibenzosuberenone **1** (1.2 eq) was dissolved under argon in dry THF and added dropwise to the reaction mixture and stirred for 1 additional hour at -78°C. Then, the reaction was allowed to warm up to room temperature under stirring overnight. Ethanol was added to the reaction mixture to quench potential remaining *n*-BuLi and the solvent was then removed under pressure.

2nd step: Without further purification, the crude was dissolved in acetic acid and hydrochloric acid was added under stirring. The reaction mixture was refluxed (115°C) overnight under stirring. After cooling to room temperature, water was added to the reaction mixture. A green precipitate was filtered off and washed with water (3 times) and then dissolved in CH_2Cl_2 (50 mL). The organic layer was washed with water (3 times) and dried over $MgSO_4$. Solvent was then removed under reduced pressure and purified with flash chromatography on silica gel.

2.2 10-phenyl-10H-spiro[acridine-9,5'-dibenzo[a,d][7]suberene](SPA-DBS)

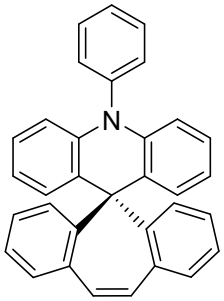

The title compound was synthesized using the general procedure

1st step: 2-bromotriphenylamine **2** (1.2 g, 3.70 mmol, 1.0 eq) in THF (20 mL), *n*-Buli (2.50 M in hexanes, 1.78 mL, 4.44 mmol, 1.2 eq) and dibenzosuberenone **1** (0.916 g, 4.44 mmol, 1.2 eq) in THF (30 mL).

2nd step: acetic acid (40 mL) and hydrochloric acid (4 mL).

After purification with flash chromatography on silica gel [column conditions: silica cartridge (24 g); solid deposit on Celite®; λdetection: (254 nm, 280 nm); gradient CH_2Cl_2/light petroleum from 10% to 20 % in 60 min at 30 mL/min], giving the title compound as a pale yellow solid (995 mg, **62**%) ^{1}H NMR (300 MHz, CD_2Cl_2) δ 7.78 – 7.66 (m, 2H), 7.64 – 7.53 (m, 1H), 7.50 – 7.43 (m, 2H), 7.29 – 7.10 (m, 6H), 7.09 – 6.97 (m, 4H), 6.83 (ddd, J = 8.6, 7.1, 1.6 Hz, 2H), 6.64 (td, J = 7.4, 1.3 Hz, 2H), 6.55 (s, 2H), 6.23 (dd, J = 8.4, 1.2 Hz, 2H). ^{13}C NMR (75 MHz, CD_2Cl_2) δ 149.53, 141.00, 137.21, 136.91, 134.81, 133.05, 131.99, 131.70, 131.27, 131.18, 130.71, 128.50, 127.94, 126.46, 125.79, 120.65, 114.13, 57.21. MALDI (m/z) calculated for $C_{33}H_{23}N$ [M]+: 433.183, found: 433.184.

2.3 spiro[dibenzo[a,d][7]suberene-5,8'-indolo[3,2,1-de]acridine](SIA-DBS)

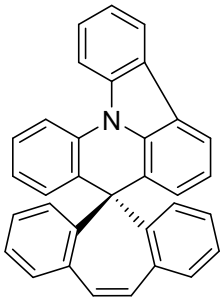

The title compound was synthesized using the general procedure

1st step: 9-(2-bromophenyl)-9H-carbazole amine **3** (1.5 g, 4.66 mmol, 1.0 eq) in THF (30 mL), *n*-Buli (2.50 M in hexanes, 2.23 mL, 5.59 mmol, 1.2 eq) and dibenzosuberenone **1** (1.15 g, 5.59 mmol, 1.2 eq) in THF (30 mL).

2nd step: acetic acid (30 mL) and hydrochloric acid (6 mL).

After purification with flash chromatography on silica gel [column conditions: silica cartridge (40 g); solid deposit on Celite®; λdetection: (254 nm, 280 nm); gradient CH_2Cl_2/light petroleum from 10% to 20 % in 120 min at 40 mL/min], giving the title compound as a colorless powder (841 mg, **42%).** ^{1}H NMR (300 MHz, CD_2Cl_2) δ 8.30 (d, J = 8.4 Hz, 1H), 8.26 – 8.16 (m, 2H), 7.84 (dd, J = 7.7, 1.1 Hz, 1H), 7.64 (ddd, J = 8.6, 7.2, 1.4 Hz, 1H), 7.45 – 7.31 (m, 4H), 7.26 – 7.12 (m, 3H), 7.08 – 6.95 (m, 3H), 6.89 – 6.79 (m, 4H), 6.62 (s, 2H). ^{13}C NMR (75 MHz, CD_2Cl_2) δ 147.81, 139.49, 138.36, 136.38, 134.71, 134.03, 133.82, 132.36, 132.32, 131.54, 131.00, 128.00, 127.36, 126.81, 126.41, 126.22, 126.01, 123.49, 122.87, 122.02, 121.05, 120.88, 117.40, 113.89, 113.20, 57.60. MALDI (m/z) calculated for $C_{33}H_{21}N$ [M]+: 431.167, found: 431.166.

2.4 spiro[dibenzo[a,d][7]suberene-5,9'-quinolino[3,2,1-kl]phenothiazine](SQPTZ-DBS)

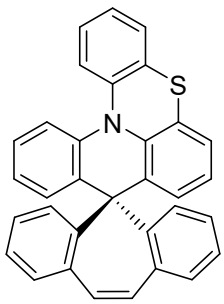

The title compound was synthesized using the general procedure

1st step: 10-(2-bromophenyl)-10H-phenothiazine **4** (1g, 2.82 mmol, 1.0 eq) in THF (20 mL), *n*-Buli (2.50 M in hexanes, 1.35 mL, 3.39 mmol, 1.2 eq) and dibenzosuberenone **1** (0.699 g, 3.39 mmol, 1.2 eq) in THF (30 mL).

2nd step: acetic acid (30 mL) and hydrochloric acid (6 mL).

After purification with flash chromatography on silica gel [column conditions: silica cartridge (24 g); solid deposit on Celite®; λdetection: (254 nm, 280 nm); gradient CH_2Cl_2/light petroleum from 10% to 20% in 90 min at 30 mL/min], giving the title compound as a colorless powder (532 mg, **41%**). ^{1}H NMR (300 MHz, CD_2Cl_2) δ 7.41 – 7.38 (m, 1H), 7.38 – 7.35 (m, 1H), 7.31 – 7.27 (m, 1H), 7.26 – 6.99 (m, 11H), 6.96 – 6.82 (m, 4H), 6.81 – 6.76 (m, 1H), 6.56 (s, *J* = 0.9 Hz, 2H). ^{13}C NMR (75 MHz, CD_2Cl_2) δ 148.50, 145.13, 143.41, 140.12, 138.41, 138.12, 136.71, 134.56, 134.05, 133.73, 132.78, 132.68, 132.20, 131.89, 131.04, 131.00, 130.82, 128.62, 128.50, 127.53, 127.33, 127.25, 126.58, 126.41, 126.11, 125.58, 124.40, 124.28, 124.06, 123.18, 120.37, 118.65, 57.38. MALDI (m/z) calculated for $C_{33}H_{21}NS$ [M]+: 463.139, found: 463.138.

2.5 spiro[dibenzo[a,d][7]suberene-5,9'-fluorene] (SF-DBS)

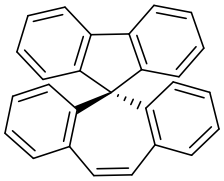

The title compound was synthesized using the general procedure

1st step : 2-iodo-1,1'-biphenyl (0.90 g, 3.20 mmol, 1.0 eq) in THF (10 mL), *n*-BuLi (2.50 M in pentane, 1.28 mL, 3.20 mmol, 1.0 eq), dibenzosuberenone **1** (0.62 g, 3.20 mmol, 1.0 eq) in THF (20 mL)

2nd step: After purification with flash chromatography on silica gel. [column conditions: Silica cartridge 24 g ; solid deposit on Celite®; λdetection: (254 nm, 280 nm); ethyl acetate in light petroleum at 40 mL/min (26 min / 1%->4%; 10 min / 70%; 10 min / 100%)] to give a colorless solid (0.87 g, **85 %**) ^{1}H NMR (300 MHz, CD_2Cl_2) δ 7.97 (ddd, J = 7.8, 1.1, 0.7 Hz, 2H), 7.78 (ddd, J = 7.6, 1.3, 0.7 Hz, 2H), 7.41 (dd, J = 7.6, 1.1 Hz, 2H), 7.39 (dd, J = 7.7, 1.6, 2H), 7.30 – 7.25 (m, 2H), 7.25 – 7.19 (m, 2H), 6.97 (s, 2H), 6.99 – 6.93 (m, 2H), 6.88 (dd, J = 8.2, 1.5 Hz, 2H). ^{13}C NMR (75 MHz, CD_2Cl_2) δ 153.5, 142.3, 139.4, 137.0, 133.8, 132.9, 129.2, 128.9, 128.6, 128.1, 127.9, 127.5, 120.8, 66.6. HRMS ASAP (m/z) calculated for $C_{27}H_{19}$ $[M+H]^+$: 343.14868; found : 343.1488.

These data are consistent with previously reported data.[18]

3 Molecular structures of SPA-F, SIA-F and SQPTZ-F

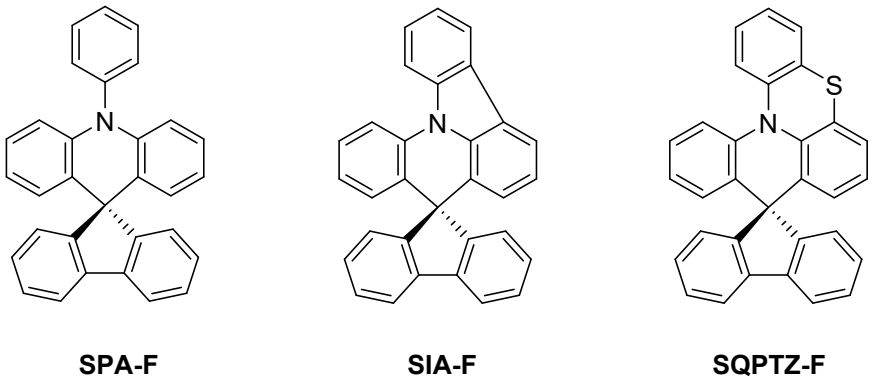

*Figure S 1 Structures of **SPA-F**, **SIA-F** and **SQPTZ-F***

All relevant information for synthetic procedures and characterizations can be found in the literature[16, 19-20]

4 Thermal Properties

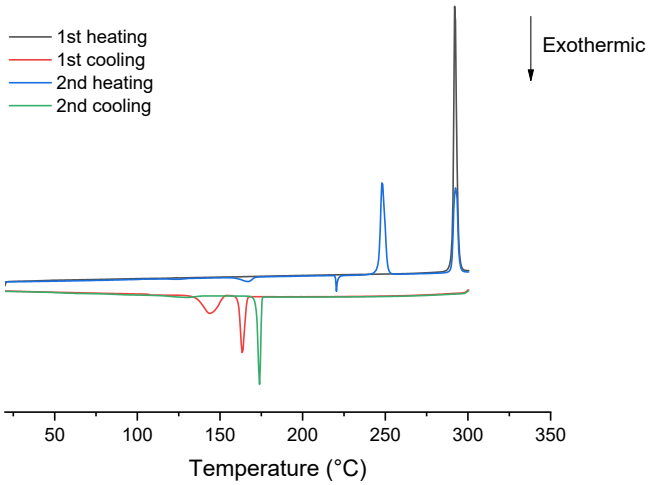

*Figure S 2 DSC curves of **SPA-DBS***

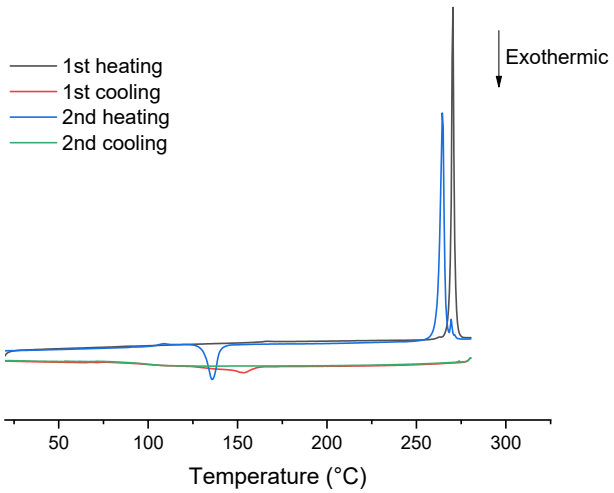

*Figure S 3 DSC curves of **SIA-DBS***

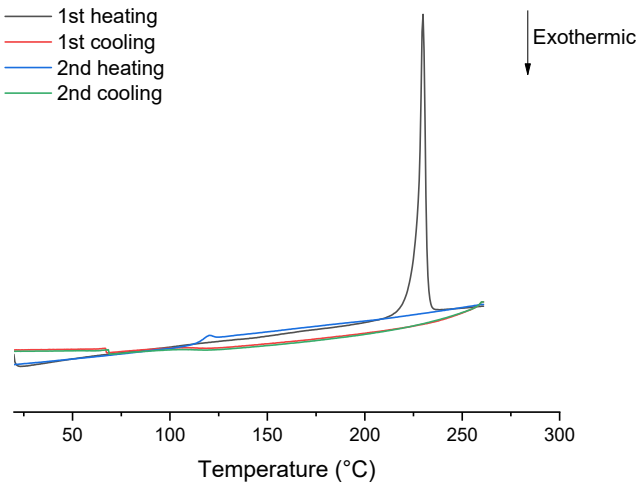

*Figure S 4 DSC curves of **SQPTZ-DBS***

5 Photophysical properties

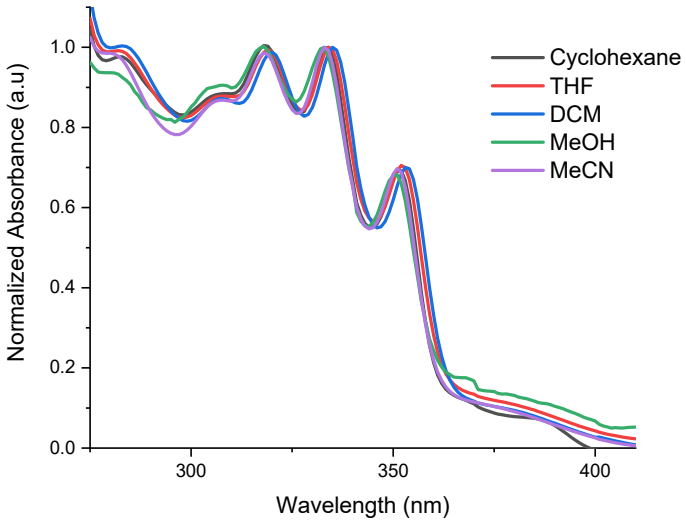

*Figure S 5 Absorption spectra of **SPA-DBS** in various solvents*

*Table S 1 Lippert-Mataga formalism calculation of **SPA-DBS** in various solvents*

solvent	λ_{abs} (nm)	λ_{em} (nm)	ν_{abs} (cm^{-1})	ν_{em} (cm^{-1})	$\Delta\nu$ (cm^{-1})	ε ($F.m^{-1}$)	n	Δf
cyclohexane	352	401	28409.09	24937.66	3471.44	2.02	1.426	-0.0016
DCM	353	457	28328.61	21881.84	6446.77	8.93	1.424	0.2172
THF	352	443	28409.09	22573.36	5835.73	7.58	1.407	0.2096
ACN	351	472	28490.03	21186.44	7303.59	37.5	1.344	0.3055
methanol	351	452	28490.03	22123.89	6366.13	37.2	1.328	0.3114

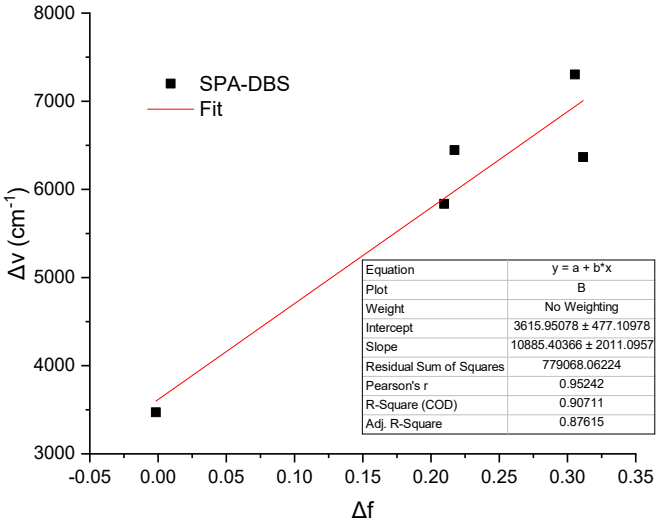

*Figure S 6 Lippert-Mataga formalism linear fit for **SPA-DBS***

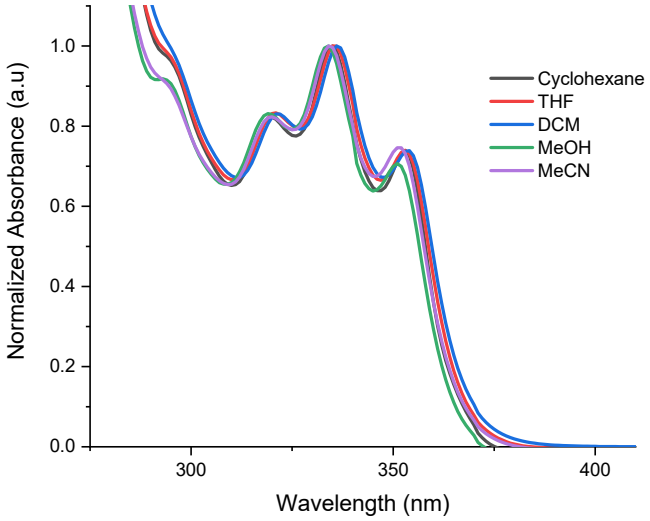

*Figure S 7 Absorption spectra of **SIA-DBS** in various solvents*

*Table S 2 Lippert-Mataga formalism calculation of **SIA-DBS** in various solvents*

solvent	λ_{abs} (nm)	λ_{em} (nm)	ν_{abs} (cm^{-1})	ν_{em} (cm^{-1})	$\Delta\nu$ (cm^{-1})	E ($F.m^{-1}$)	n	Δf
cyclohexane	353	375	28328.61	26666.67	1661.95	2.02	1.426	-0.0016
DCM	354	425	28248.59	23529.41	4719.18	8.93	1.424	0.2172
THF	353	417	28328.61	23980.82	4347.80	7.58	1.407	0.2096
ACN	351	441	28490.03	22675.74	5814.29	37.5	1.344	0.3055
methanol	351	433	28490.03	23094.69	5395.34	37.2	1.328	0.3114

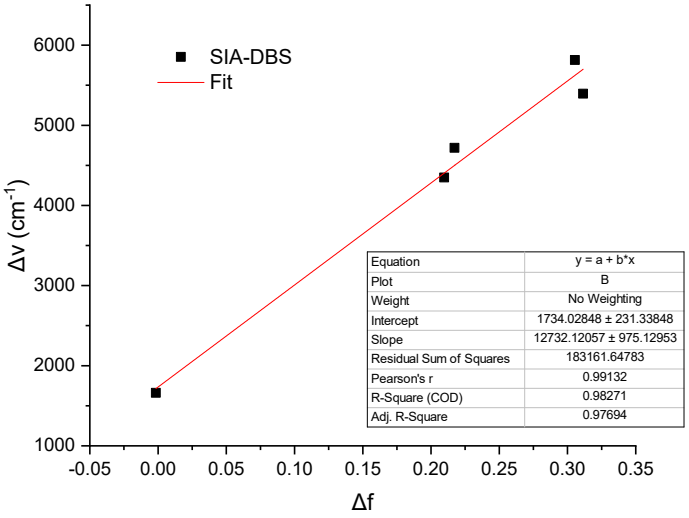

*Figure S 8 Lippert-Mataga formalism linear fit for **SIA-DBS***

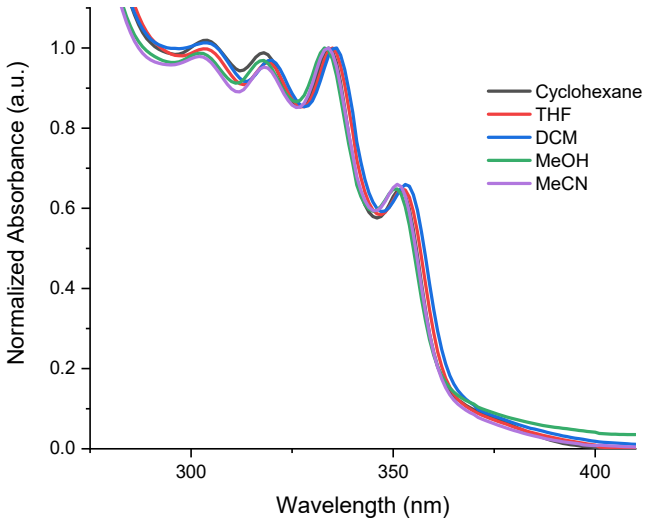

*Figure S 9 Absorption spectra of **SQPTZ-DBS** in various solvents*

*Table S 3 Lippert-Mataga formalism calculation of **SQPTZ-DBS** in various solvents*

solvent	λ_{abs} (nm)	λ_{em} (nm)	ν_{abs} (cm^{-1})	ν_{em} (cm^{-1})	$\Delta\nu$ (cm^{-1})	E ($F.m^{-1}$)	n	Δf
cyclohexane	352	417	28409.09	23980.82	4428.28	2.02	1.426	-0.0016
DCM	353	485	28328.61	20618.56	7710.06	8.93	1.424	0.2172
THF	352	475	28409.09	21052.63	7356.46	7.58	1.407	0.2096
ACN	351	518	28490.03	19305.02	9185.01	37.5	1.344	0.3055
methanol	351	499	28490.03	20040.08	8449.95	37.2	1.328	0.3114

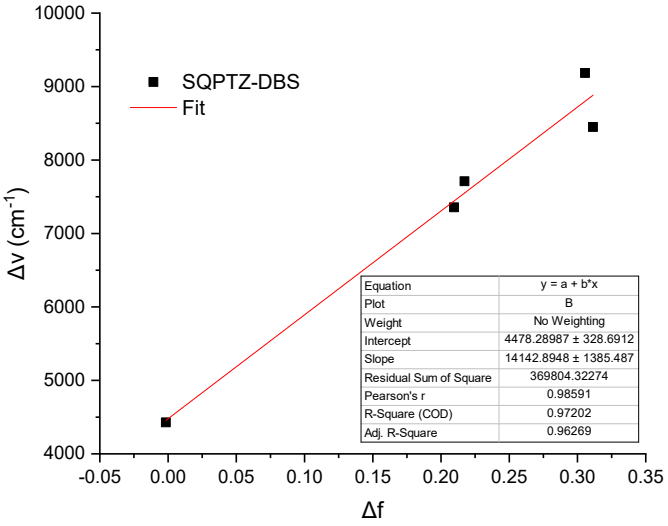

*Figure S 10 Lippert-Mataga formalism linear fit for **SQPTZ-DBS***

Table S 4 Summary of the radius of the solvation sphere (r), dipole moment at the ground (μ) and excited (μ) states and the difference (Δμ) for **SPA-DBS**, **SIA-DBS** and **SQPTZ-DBS***

Compound	r(Å)	Δμ (D)	μ (D)	μ* (D)
SPA-DBS	6.3	16.3	2.2	18.5
SIA-DBS	5.9	15.9	0.6	16.5
SQPTZ-DBS	6.1	17.9	1.4	19.3

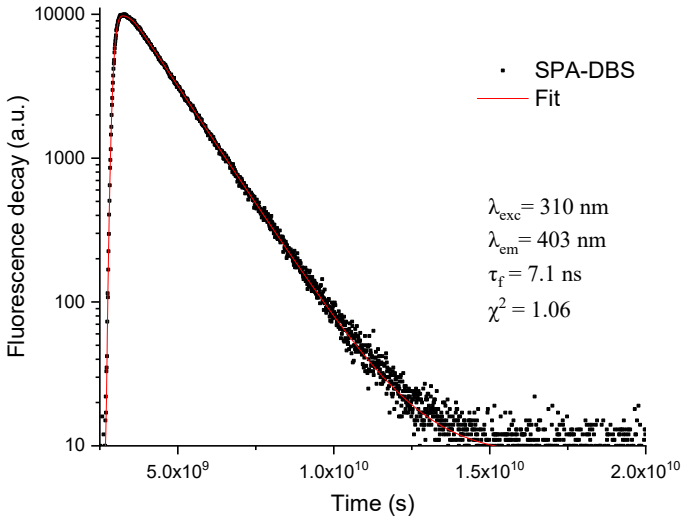

*Figure S 11 Fluorescence decay of **SPA-DBS** in cyclohexane*

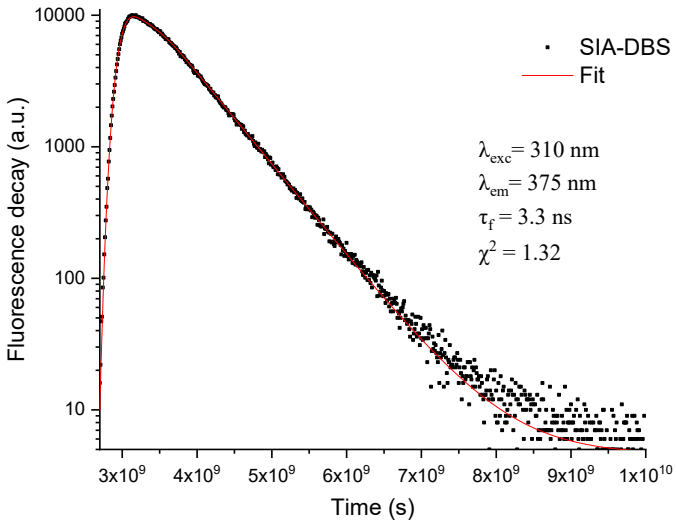

*Figure S 12 Fluorescence decay of **SIA-DBS** in cyclohexane*

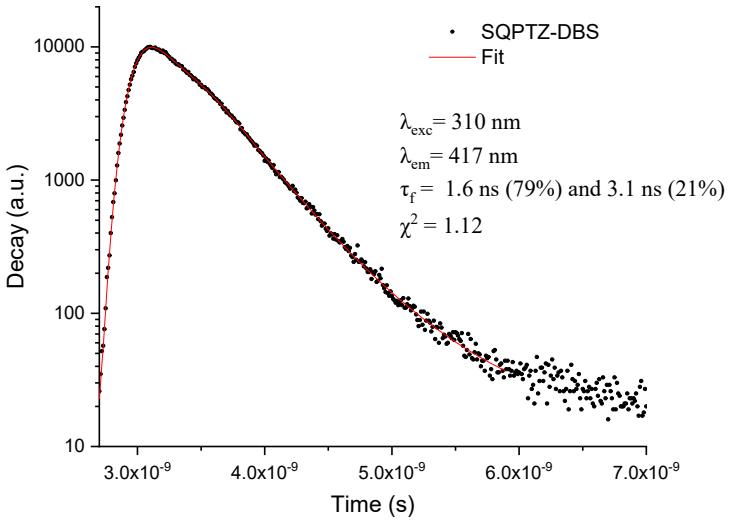

*Figure S 13 Fluorescence decay of **SQPTZ-DBS** in cyclohexane*

6 Molecular modelling

λ (nm)	Oscillator Strength	Major contributions	Minor contributions
395	0.004	HOMO→LUMO (99%)	
355	0.194	H-1→LUMO (97%)	
339	0.024	H-2→LUMO (32%), HOMO→L+1 (64%)	
~~**λ (nm)**~~	~~**Oscillator Strength**~~	~~**Major contributions**~~	~~**Minor contributions**~~
422	0.008	HOMO→→LUMO (99%)	
354	0.189	H-1→LUMO (97%)	
348	0.000	HOMO→L+1 (99%)	
339	0.000	HOMO→L+2 (99%)	
321	0.021	H-2→LUMO (75%), HOMO→L+4 (14%)	H-1→L+3 (9%)
309	0.000	HOMO→L+3 (100%)	
306	0.074	H-2→LUMO (12%), HOMO→L+4 (80%)	H-1→L+3 (2%)
295	0.041	H-4→LUMO (21%), HOMO→L+5 (76%)	
291	0.032	H-3→LUMO (72%), H-1→L+5 (21%)	H-1→L+7 (2%)
283	0.003	H-1→L+2 (98%)	
283	0.048	H-4→LUMO (64%), HOMO→L+5 (20%), HOMO→L+8 (13%)	
283	0.003	H-1→L+1 (99%)	
277	0.000	H-1→L+4 (99%)	
277	0.088	H-2→LUMO (11%), H-1→L+3 (79%)	H-9→LUMO (3%)
273	0.015	HOMO→L+7 (71%), HOMO→L+8 (23%)	H-4→LUMO (2%)
272	0.001	HOMO→L+6 (96%)	HOMO→L+12 (2%)
266	0.208	H-4→LUMO (10%), HOMO→L+7 (24%), HOMO→L+8 (58%)	H-2→L+4 (3%)
265	0.002	H-5→LUMO (94%)	H-2→L+2 (2%)
260	0.262	H-3→LUMO (18%), H-1→L+5 (74%)	

*Table S 5 TD-DFT results of **SPA-DBS** (B3LYP/6-311+g(d,p)).*

*Table S 6 TD-DFT results of **SIA-DBS** (B3LYP/6-311+g(d,p)).*

λ (nm)	Oscillator Strength	Major contributions	Minor contributions
329	0.063	H-2→LUMO (65%), HOMO→L+1 (31%)	H-1→L+2 (3%), H-1→L+3 (9%), HOMO→L+2 (6%)
309	0.024	H-3→LUMO (75%), HOMO→LUMO (9%)	
418	0.014		
306	0.004	H-1→L+1 (97%)	
297	0.034	HOMO→L+2 (59%), HOMO→L+3 (18%)	H-3→LUMO (4%), HOMO→L+4 (6%)
293	0.002	HOMO→L+2 (22%), HOMO→L+3 (69%)	H-4→LUMO (6%)
290	0.032	H-4→LUMO (68%), H-1→L+5 (16%)	H-1→L+4 (3%), HOMO→L+3 (6%)
289	0.065	H-2→L+1 (32%), HOMO→L+4 (53%)	HOMO→L+5 (7%), HOMO→L+6 (3%)
282	0.135	H-2→L+1 (24%), HOMO→L+4 (35%), HOMO→L+5 (27%)	HOMO→L+2 (4%), HOMO→L+3 (2%), HOMO→L+6 (4%)
277	0.016	H-1→L+2 (81%)	H-3→LUMO (4%), H-1→L+3 (4%), H-1→L+4 (7%)
274	0.084	H-3→LUMO (13%), H-1→L+3 (76%)	H-8→LUMO (3%)
269	0.224	H-2→L+1 (22%), HOMO→L+5 (59%), HOMO→L+6 (10%)	
266	0.082	H-1→L+4 (83%)	H-1→L+2 (7%)
265	0.045	H-5→LUMO (12%) H-3→L+1 (58%), H-2→L+4 (13%)	H-2→L+2 (5%)
264	0.046	H-5→LUMO (77%), H-3→L+1 (12%)	H-1→L+4 (2%)
260	0.002	H-3→L+1 (14%), H-2→L+2 (56%), H-2→L+4 (15%)	H-6→L+1 (3%), HOMO→L+6 (6%)
257	0.002	H-2→L+2 (30%), H-2→L+4 (56%)	H-3→L+1 (4%)
257	0.036	H-2→L+3 (69%), H-1→L+5 (23%)	H-4→LUMO (4%)

*Table S 7 TD-DFT results of **SQPTZ-DBS** (B3LYP/6-311+g(d,p)).*

354	0.182	H-1→LUMO (97%)	
342	0.016	HOMO→L+1 (88%)	H-2→LUMO (3%), HOMO→L+2 (5%)
331	0.011	H-2→LUMO (83%)	HOMO→L+2 (6%), HOMO→L+3 (5%)
326	0.007	HOMO→L+2 (66%), HOMO→L+3 (14%)	H-2→LUMO (7%), HOMO→L+1 (8%)
308	0.038	H-3→LUMO (76%)	H-1→L+2 (6%), H-1→L+3 (6%), H-1→L+4 (2%), HOMO→L+3 (3%)
307	0.051	HOMO→L+2 (19%), HOMO→L+3 (73%)	H-3→LUMO (2%)
301	0.098	HOMO→L+4 (76%), HOMO→L+5 (14%)	
294	0.007	H-4→LUMO (37%), H-1→L+1 (44%)	H-1→L+5 (5%), H-1→L+7 (2%), HOMO→L+5 (5%)
293	0.049	HOMO→L+4 (15%), HOMO→L+5 (58%)	H-2→L+1 (4%), H-1→L+1 (7%), HOMO→L+7 (6%)
289	0.024	H-4→LUMO (32%), H-1→L+1 (42%)	H-1→L+2 (5%), H-1→L+4 (8%), H-1→L+7 (3%), HOMO→L+6 (4%)
287	0.005	HOMO→L+6 (81%)	H-5→LUMO (4%), H-4→LUMO (2%), H-3→L+1 (2%)
279	0.073	H-5→LUMO (13%), H-1→L+2 (27%), H-1→L+3 (14%), HOMO→L+7 (19%)	H-3→LUMO (8%), H-1→L+4 (2%), HOMO→L+5 (6%), HOMO→L+6 (3%)
277	0.028	H-2→L+1 (15%), HOMO→L+7 (48%)	H-5→LUMO (5%), H-3→LUMO (4%), H-1→L+2 (9%), H-1→L+3 (5%), HOMO→L+5 (8%)
273	0.033	H-5→LUMO (15%), H-2→L+1 (52%), HOMO→L+7 (15%)	H-1→L+2 (9%)
272	0.043	H-5→LUMO (40%), H-2→L+1 (19%), H-1→L+2 (16%)	H-6→LUMO (3%), H-4→LUMO (4%), H-1→L+4 (2%), HOMO→L+6 (4%), HOMO→L+7 (5%)

269	0.027	H-1→L+2 (22%), H-1→L+3 (61%)	H-5→LUMO (9%), H-1→L+6 (2%)
266	0.115	H-1→L+4 (73%)	H-5→LUMO (4%), H-4→LUMO (5%), H-1→L+1 (2%), H-1→L+3 (5%), H-1→L+5 (4%)
264	0.056	H-6→LUMO (36%), H-2→L+2 (39%)	H-2→L+1 (3%), H-2→L+3 (7%)
260	0.034	H-6→LUMO (23%), HOMO→L+8 (26%), HOMO→L+10 (22%)	H-2→L+3 (7%), HOMO→L+9 (8%)

*Table S 8 Atomic coordinates of **SPA-DBS** after geometry optimization (B3LYP /6-31g(d))*

Atom	X (Å)	Y (Å)	Z (Å)
C	-6.2213	-1.0551	0.0014
C	-4.8529	-0.4263	-0.0652
C	-4.6927	0.918	-0.0379
N	-5.6904	1.7501	-0.0028
C	-6.9231	1.3401	0.0339
C	-7.2652	0.0304	0.065
C	-5.4497	3.023	-0.0045
C	-8.0061	2.1473	-0.1078
C	-9.286	1.7456	-0.0658
C	-9.5714	0.4492	0.0766
C	-8.5409	-0.4002	0.1113
C	-6.1139	3.8994	0.7851
C	-5.8723	5.22	0.7957
C	-4.9361	5.7396	-0.0079
C	-4.2547	4.9122	-0.8098
C	-4.5118	3.5946	-0.796
C	-3.8228	-1.2935	-0.1096
C	-2.5532	-0.8792	-0.077
C	-2.345	0.4322	0.0614
C	-3.3895	1.274	0.1017
C	-6.2812	-1.7471	1.3614
C	-6.5196	-3.0536	1.5987
C	-6.7522	-4.0029	0.6757
C	-6.8217	-3.992	-0.6619
C	-6.6839	-3.0279	-1.5886
C	-6.4195	-1.7255	-1.3563
C	-6.8301	-3.4379	-2.8703
C	-6.7242	-2.6121	-3.9194
C	-6.462	-1.322	-3.6946
C	-6.3165	-0.9088	-2.4296
C	-6.0716	-0.9469	2.4317

C	-6.0868	-1.3806	3.6982
C	-6.3221	-2.6749	3.9278
C	-6.5335	-3.4843	2.8818
H	-7.9353	3.223	-0.3302
H	-10.1101	2.4701	-0.1848
H	-10.613	0.09	0.0939
H	-8.7643	-1.4798	0.1503
H	-6.8462	3.5499	1.5354
H	-6.4281	5.8809	1.4824
H	-4.7314	6.8227	-0.0092
H	-3.4963	5.3229	-1.4979
H	-3.958	3.0001	-1.5451
H	-4.0095	-2.3801	-0.1454
H	-1.7148	-1.5942	-0.0928
H	-1.313	0.8058	0.1786
H	-3.0621	2.3018	0.3208
H	-6.928	-5.0239	1.0747
H	-7.0389	-5.0065	-1.0571
H	-7.0475	-4.4909	-3.1254
H	-6.8497	-2.9837	-4.9501
H	-6.3683	-0.6159	-4.5364
H	-6.1016	0.1652	-2.3048
H	-5.8735	0.1298	2.303
H	-5.9095	-0.6874	4.5373
H	-6.3414	-3.0632	4.9598
H	-6.7227	-4.5418	3.1409

Number of imaginary frequency: 0

*Table S9 Atomic coordinates of **SIA-DBS** after geometry optimization (B3LYP /6-31g(d))*

Atom	X (Å)	Y (Å)	Z (Å)
C	1.05713	0.00178	0.07404
C	0.06638	0.19571	-1.08283
C	-1.2993	0.08892	-0.85265
N	-1.90187	-0.21247	0.37101
C	-1.09678	-0.59122	1.46695
C	0.30782	-0.45351	1.36115
C	-3.29703	-0.13387	0.19179
C	-1.64825	-1.13036	2.64216
C	-0.84066	-1.45434	3.72707
C	0.53804	-1.25919	3.65743
C	1.09018	-0.77865	2.47455
C	-3.5563	0.1588	-1.17931
C	-4.8698	0.2929	-1.63638
C	-5.92265	0.15766	-0.7365
C	-5.66051	-0.08779	0.61838
C	-4.35908	-0.22998	1.10007
C	0.4518	0.51291	-2.3882
C	-0.49873	0.71572	-3.40088

C	-1.86587	0.61841	-3.14178
C	-2.27704	0.30389	-1.84302
C	1.63763	1.42052	0.38947
C	2.92218	1.93937	0.09991
C	4.03819	1.23475	-0.51665
C	4.19932	-0.05365	-0.86741
C	3.31166	-1.20423	-0.76364
C	1.9617	-1.20673	-0.34042
C	3.90362	-2.43113	-1.15398
C	3.21665	-3.63281	-1.15105
C	1.87942	-3.63322	-0.7551
C	1.28317	-2.44075	-0.36394
C	0.70529	2.3017	0.96982
C	0.99386	3.62628	1.27647
C	2.26444	4.13159	1.00453
C	3.19812	3.29061	0.42351
H	-2.70684	-1.33405	2.6983
H	-1.29643	-1.86602	4.62333
H	1.17716	-1.4969	4.50251
H	2.16722	-0.65988	2.39498
H	-5.06171	0.51238	-2.68337
H	-6.94821	0.25948	-1.07933
H	-6.48687	-0.1617	1.32006
H	-4.20423	-0.36899	2.16076
H	1.50865	0.60915	-2.62055
H	-0.15856	0.96175	-4.40278
H	-2.59211	0.79019	-3.93146
H	4.89723	1.87589	-0.70595
H	5.16879	-0.29799	-1.29787
H	4.94411	-2.41337	-1.46852
H	3.71074	-4.55035	-1.45826
H	1.29919	-4.55173	-0.75159
H	0.24115	-2.46919	-0.06611
H	-0.29289	1.9406	1.18788
H	0.22747	4.25446	1.72187
H	2.51986	5.16183	1.23623
H	4.19196	3.67123	0.20148

Number of imaginary frequency: 0

*Table S10 Atomic coordinates of **SQPTZ-DBS** after geometry optimization (B3LYP /6-31g(d))*

Atom	X (Å)	Y (Å)	Z (Å)
C	1.24237	0.05092	-0.06764
C	0.27218	-0.80022	-0.91767
C	-1.0635	-1.00309	-0.54337
N	-1.62391	-0.34733	0.58349
C	-0.74698	0.15529	1.57963
C	0.61025	0.38223	1.30202
C	-2.94827	0.17183	0.45947

C	-1.24043	0.38609	2.87707
C	-0.41749	0.90478	3.86743
C	0.92328	1.1834	3.58521
C	1.42249	0.90589	2.31859
C	-3.94377	-0.61575	-0.14375
C	-5.24353	-0.1268	-0.29595
C	-5.57605	1.14408	0.1694
C	-4.58667	1.94322	0.74458
C	-3.28111	1.47234	0.87047
C	0.74748	-1.42375	-2.07919
C	-0.07088	-2.2346	-2.85673
C	-1.3915	-2.46185	-2.4651
C	-1.87692	-1.86664	-1.30386
S	-3.51635	-2.24922	-0.71215
C	1.41865	1.41189	-0.81985
C	2.61009	2.10165	-1.1494
C	3.97904	1.66626	-0.90779
C	4.4815	0.52562	-0.40277
C	3.83402	-0.67655	0.10439
C	2.44607	-0.90035	0.2548
C	4.73384	-1.6992	0.49787
C	4.31519	-2.90411	1.0342
C	2.94679	-3.11796	1.2028
C	2.05	-2.12999	0.81764
C	0.20273	2.03695	-1.1567
C	0.12625	3.27267	-1.78819
C	1.30053	3.94909	-2.11519
C	2.51097	3.36012	-1.79293
H	-2.27786	0.1556	3.09459
H	-0.82012	1.08042	4.8612
H	1.57536	1.59534	4.34984
H	2.4706	1.09082	2.10168
H	-5.98948	-0.75126	-0.77912
H	-6.59283	1.51164	0.06687
H	-4.82352	2.94713	1.08574
H	-2.51708	2.10743	1.30426
H	1.78279	-1.26619	-2.3666
H	0.31716	-2.69758	-3.75915
H	-2.04335	-3.10495	-3.04873
H	4.72139	2.40142	-1.21305
H	5.56812	0.47741	-0.36112
H	5.79734	-1.51391	0.3695
H	5.04025	-3.66023	1.32218
H	2.57576	-4.04457	1.63168
H	0.99203	-2.31932	0.96219
H	-0.72924	1.5408	-0.91659
H	-0.84628	3.69795	-2.0199
H	1.27248	4.91576	-2.6102
H	3.43569	3.87454	-2.04207

Number of imaginary frequency: 0

7 Devices

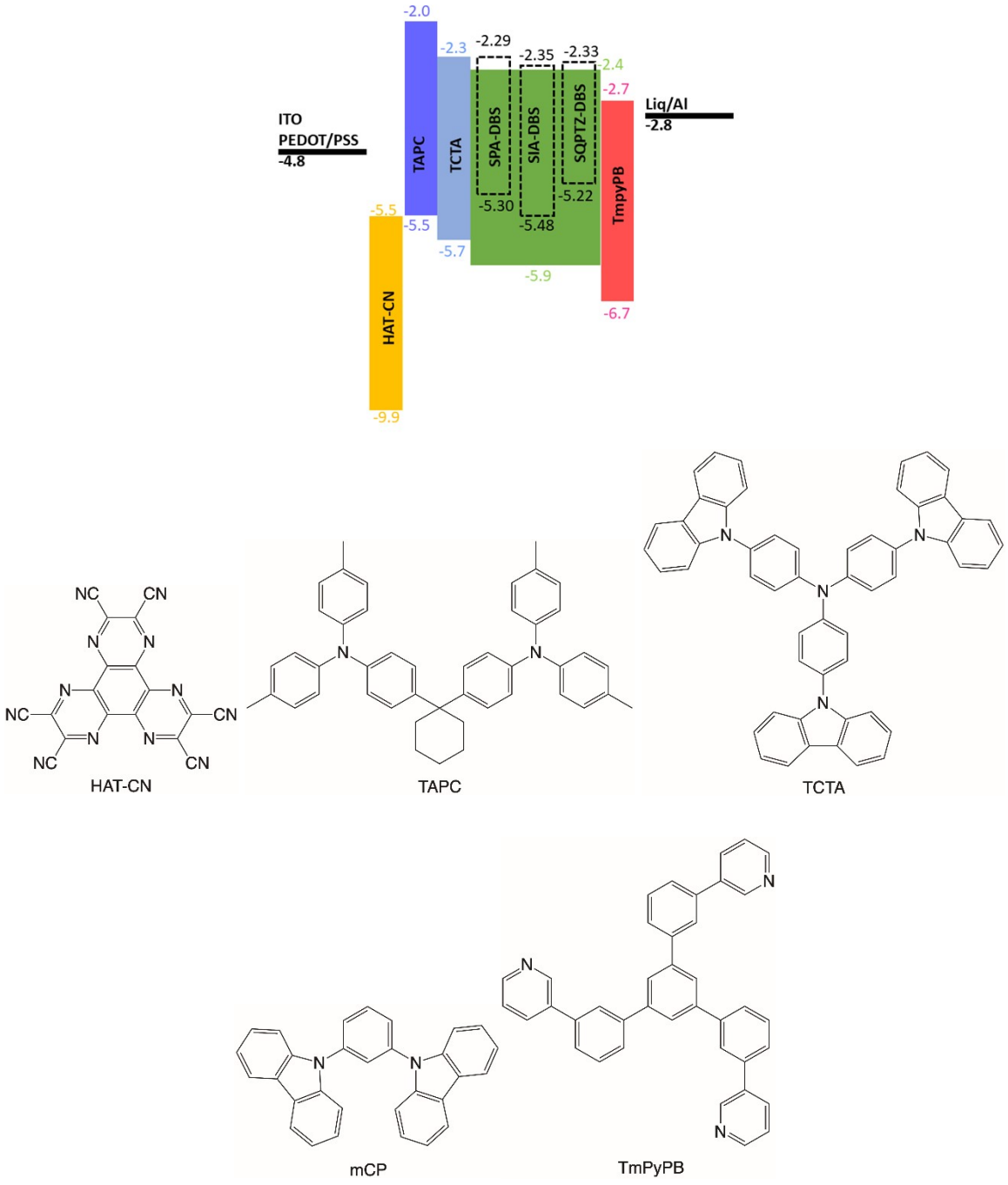

Figure S 14 The energy level alignment of the device and the molecular structures of materials in different layers, 1,4,5,8,9,11-hexaazatriphenylenehexacarbonitrile (HAT-CN); 1,1-bis[(di-4-tolylamino)phenyl]cyclohexane (TAPC); 4,4',4''-tris-(carbazol-9-yl)-triphenylamine (TCTA); 1,3-di(9Hcarbazol-9-yl)benzene (mCP); 1,3,5-tri[(3-pyridyl)-phen-3-yl]benzene (TmPyPB). The LUMO/HOMO values of hosts were taken from the present CV measurements and other material were taken from literature.[21]

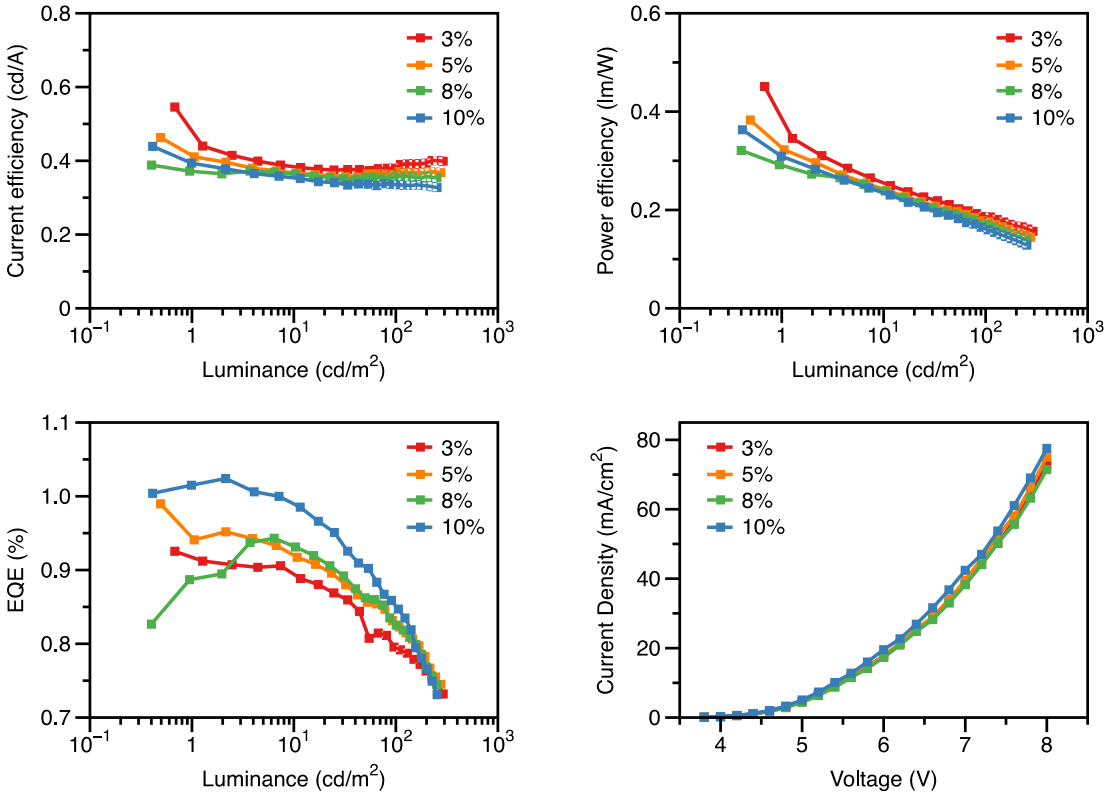

*Figure S 15 OLED device performance based on **SPA-DBS** with different doping ratios from 3 wt% to 10 wt%. a, current efficiency (CE) to luminance curve; b, power efficiency (PE) to luminance curve; c, external quantum efficiency (EQE) to luminance curve; d, current d, current density to voltage (J-V) curves.*

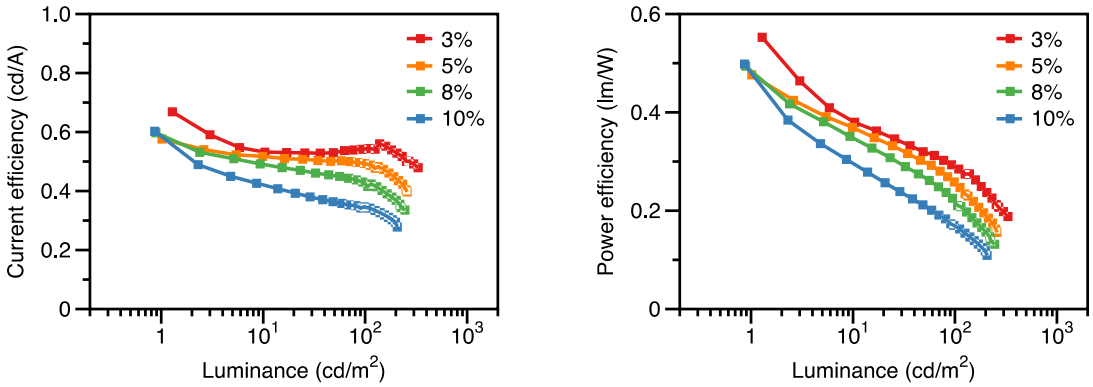

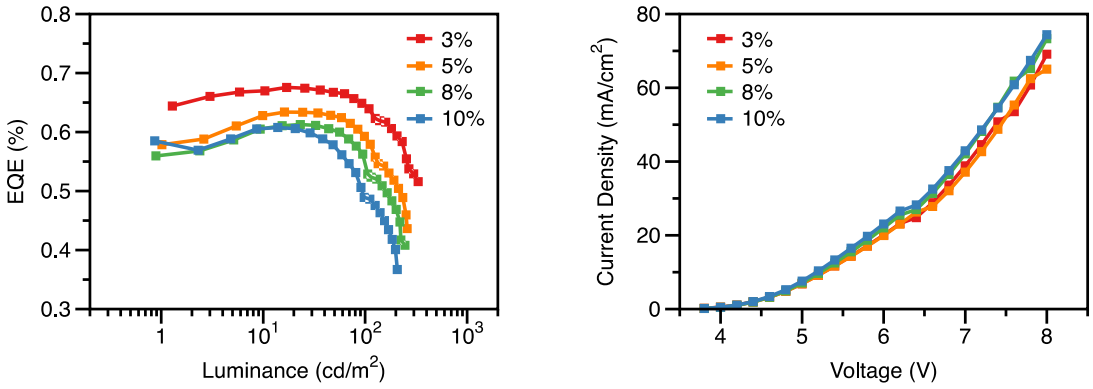

*Figure S 16 . OLED device performance based on **SIA-DBS** with different doping ratios from 3 wt% to 10 wt%. a, current efficiency (CE) to luminance curve; b, power efficiency (PE) to luminance curve; c, external quantum efficiency (EQE) to luminance curve; d, currentdensity to voltage (J-V) curves.*

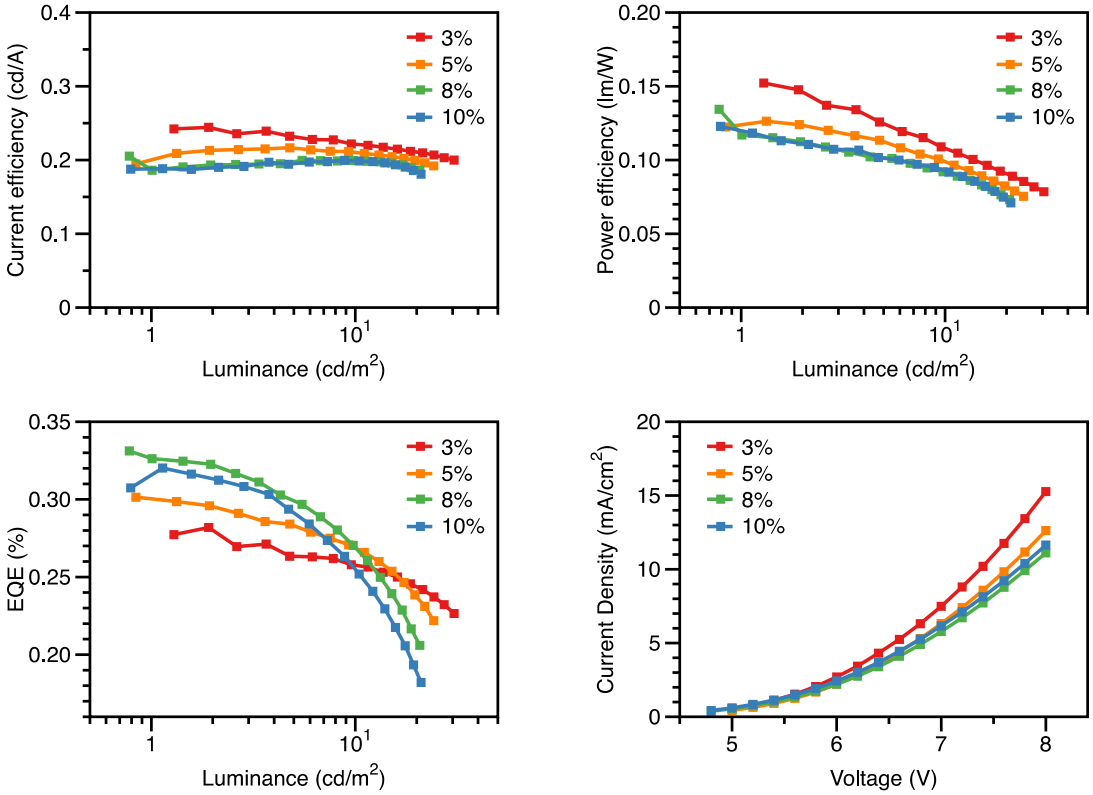

*Figure S 17 OLED device performance based on **SQPTZ-DBS** with different doping ratios from 3 wt% to 10 wt%. a, current efficiency (CE) to luminance curve; b, power efficiency (PE) to luminance curve; c, external quantum efficiency (EQE) to luminance curve; d, current density to voltage (J-V) curves.*

*Table S 11 OLED performances using **SPA-DBS**, **SIA-DBS** and **SQPTZ-DBS** as emitter with different percentage of doping and mCP as the host material.*

Emitter	V_{on} [a] (V)	CE_{max} [b] (cd/A)	PE_{max} [b] (lm/W)	EQE_{max} [b] (%)	CIE (x, y) [c]
3 wt% SPA-DBS	3.9	0.546	0.451	0.925	(0.16,0.05)
5 wt% SPA-DBS	4.0	0.463	0.383	0.990	(0.16,0.05)
8 wt% SPA-DBS	4.0	0.388	0.321	0.943	(0.16,0.05)
10 wt% SPA-DBS	4.0	0.439	0.363	1.024	(0.16,0.05)
3 wt% SIA-DBS	3.7	0.668	0.553	0.676	(0.24,0.14)
5 wt% SIA-DBS	3.8	0.576	0.476	0.634	(0.24,0.14)
8 wt% SIA-DBS	3.8	0.597	0.494	0.613	(0.23,0.15)
10 wt% SIA-DBS	3.8	0.603	0.498	0.608	(0.23,0.13)
3 wt% SQPTZ-DBS	5.0	0.244	0.152	0.282	(0.19,0.10)
5 wt% SQPTZ-DBS	5.0	0.217	0.126	0.301	(0.19,0.10)
8 wt% SQPTZ-DBS	5.0	0.205	0.134	0.331	(0.18,0.10)
10 wt% SQPTZ-DBS	5.0	0.200	0.123	0.320	(0.18,0.10)

a) Recorded at a luminance of 1 cd/m^2. b) The maximum CE, PE and EQE. c) Measured at a driving current density of 5 mA/cm^2.

8 X-ray diffraction structures and tables

8.1 SPA-DBS

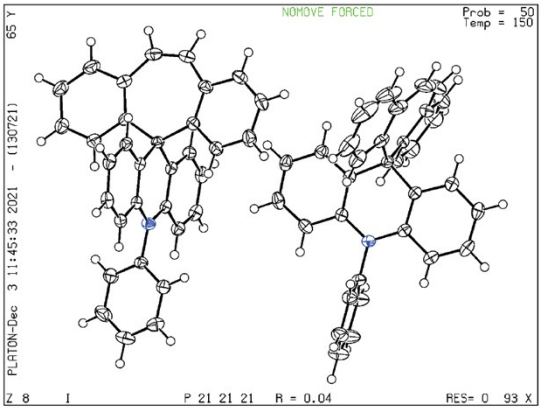

*Figure S 18 Ellipsoid plot of **SPA-DBS***

*Table S 12 Crystal data and structure refinement for **SPA-DBS***

Identification code	shelx
Empirical formula	C33 H23 N
Formula weight	433.52
Temperature	150(2) K
Wavelength	0.71073 Å
Crystal system	Orthorhombic
Space group	P 2_1 2_1 2_1
Unit cell dimensions	a = 12.2037(14) Å α= 90°.
	b = 14.530(2) Å β= 90°.
	c = 25.417(3) Å γ = 90°.
Volume	4506.9(10) $Å^3$
Z	8
Density (calculated)	1.278 Mg/m^3
Absorption coefficient	0.073 mm^{-1}
F(000)	1824
Crystal size	0.23 x 0.21 x 0.02 mm^3
Theta range for data collection	2.705 to 27.470°.
Index ranges	-14<=h<=15, -18<=k<=18, -32<=l<=32
Reflections collected	35721
Independent reflections	10250 [R(int) = 0.0559]
Completeness to theta = 25.242°	99.8 %
Refinement method	Full-matrix least-squares on F^2
Data / restraints / parameters	10250 / 0 / 614
Goodness-of-fit on F^2	1.021
Final R indices [I>2sigma(I)]	R1 = 0.0444, wR2 = 0.1086
R indices (all data)	R1 = 0.0556, wR2 = 0.1157
Absolute structure parameter	0(4)
Extinction coefficient	n/a
Largest diff. peak and hole	0.170 and -0.246 $e.Å^{-3}$

8.2 SIA-DBS

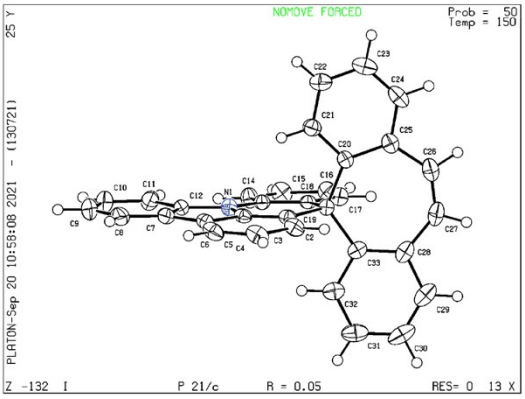

*Figure S 19 Ellipsoid plot of **SIA-DBS***

*Table S 13 Crystal data and structure refinement for **SIA-DBS***

Identification code	shelx
Empirical formula	C33 H21 N
Formula weight	431.51
Temperature	150(2) K
Wavelength	0.71073 Å
Crystal system	Monoclinic
Space group	P 2_1/c
Unit cell dimensions	a = 9.6276(13) Å α= 90°.
	b = 14.233(2) Å β= 93.470(4)°.
	c = 15.873(2) Å γ = 90°.
Volume	2171.1(5) $Å^3$
Z	4
Density (calculated)	1.320 Mg/m^3
Absorption coefficient	0.076 mm^{-1}
F(000)	904
Crystal size	0.38 x 0.24 x 0.22 mm^3
Theta range for data collection	2.119 to 27.498°.
Index ranges	-12<=h<=11, -18<=k<=18, -20<=l<=12
Reflections collected	12143
Independent reflections	4912 [R(int) = 0.0351]
Completeness to theta = 25.242°	99.5 %
Refinement method	Full-matrix least-squares on F^2
Data / restraints / parameters	4912 / 0 / 307
Goodness-of-fit on F^2	0.991
Final R indices [I>2sigma(I)]	R1 = 0.0487, wR2 = 0.1146
R indices (all data)	R1 = 0.0939, wR2 = 0.1402
Extinction coefficient	n/a
Largest diff. peak and hole	0.200 and -0.225 e.$Å^{-3}$

9 Copy of NMR Spectra

9.1 SPA-DBS – ^{1}H – CD_2Cl_2

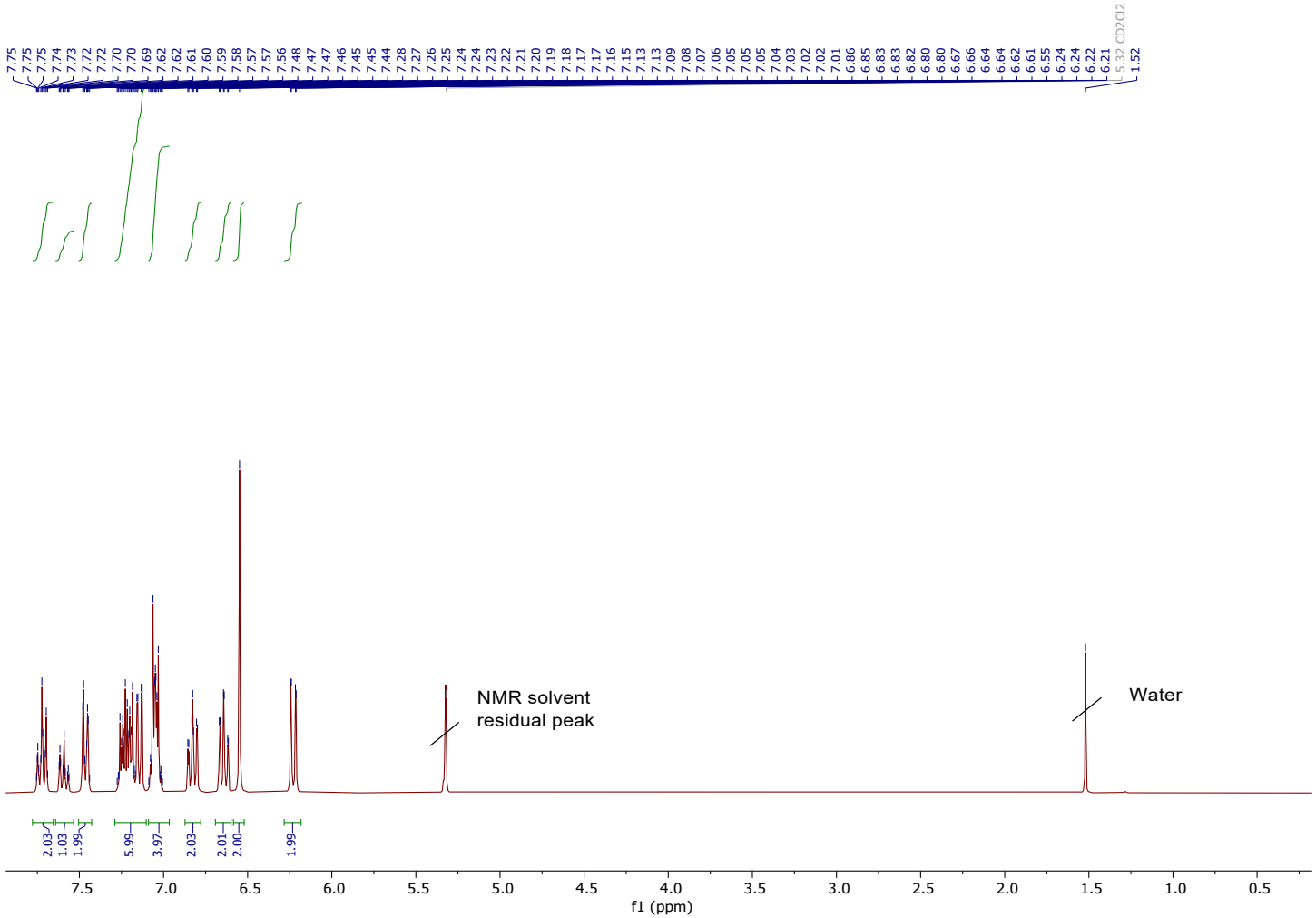

Figure S 20 ***SPA-DBS*** *– ^1H – CD_2Cl_2*

9.2 SPA-DBS – ^{13}C – CD_2Cl_2

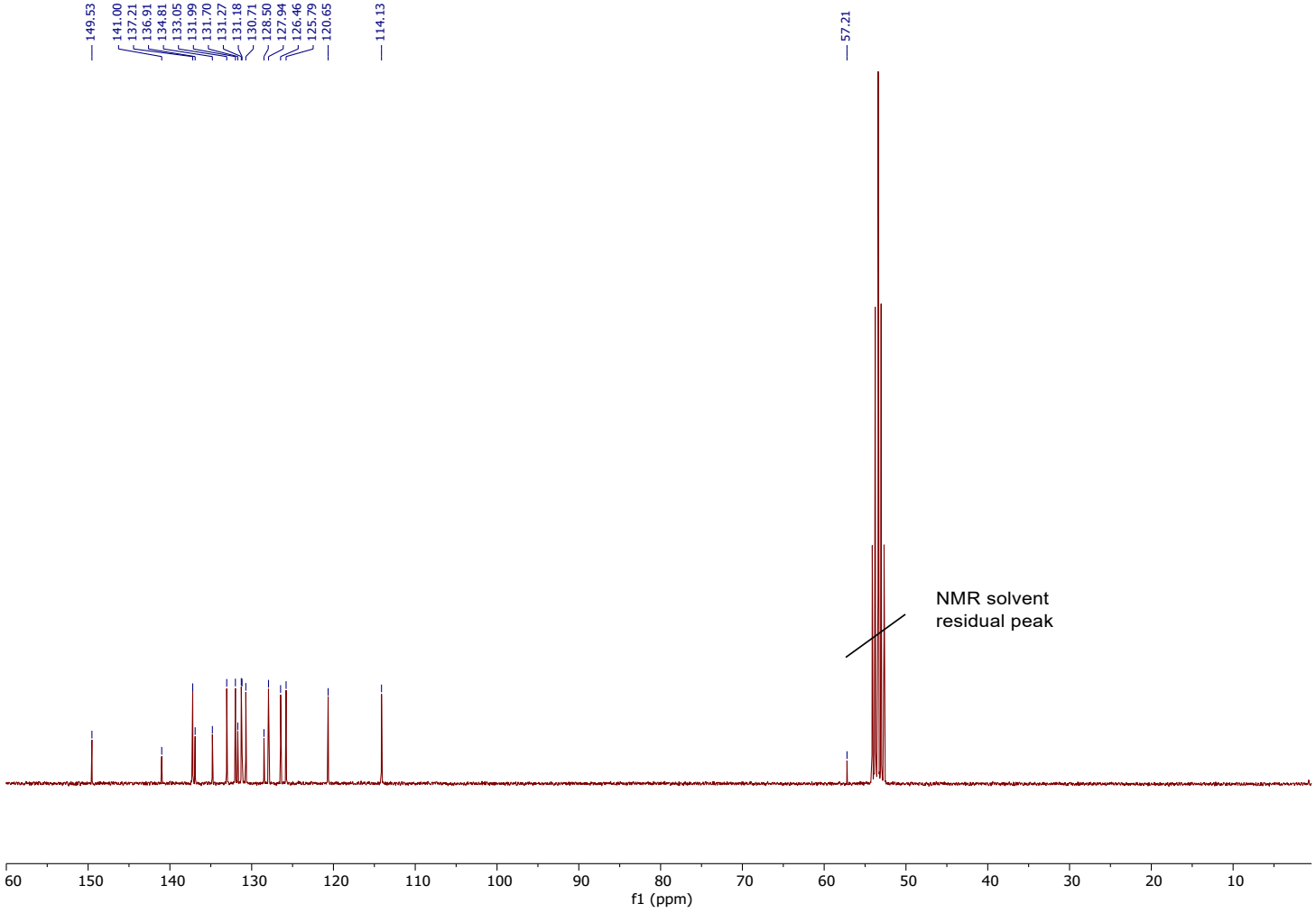

Figure S 21 ***SPA-DBS*** *– ^{13}C – CD_2Cl_2*

9.3 SPA-DBS ^{13}C-DEPT135-CD_2Cl_2

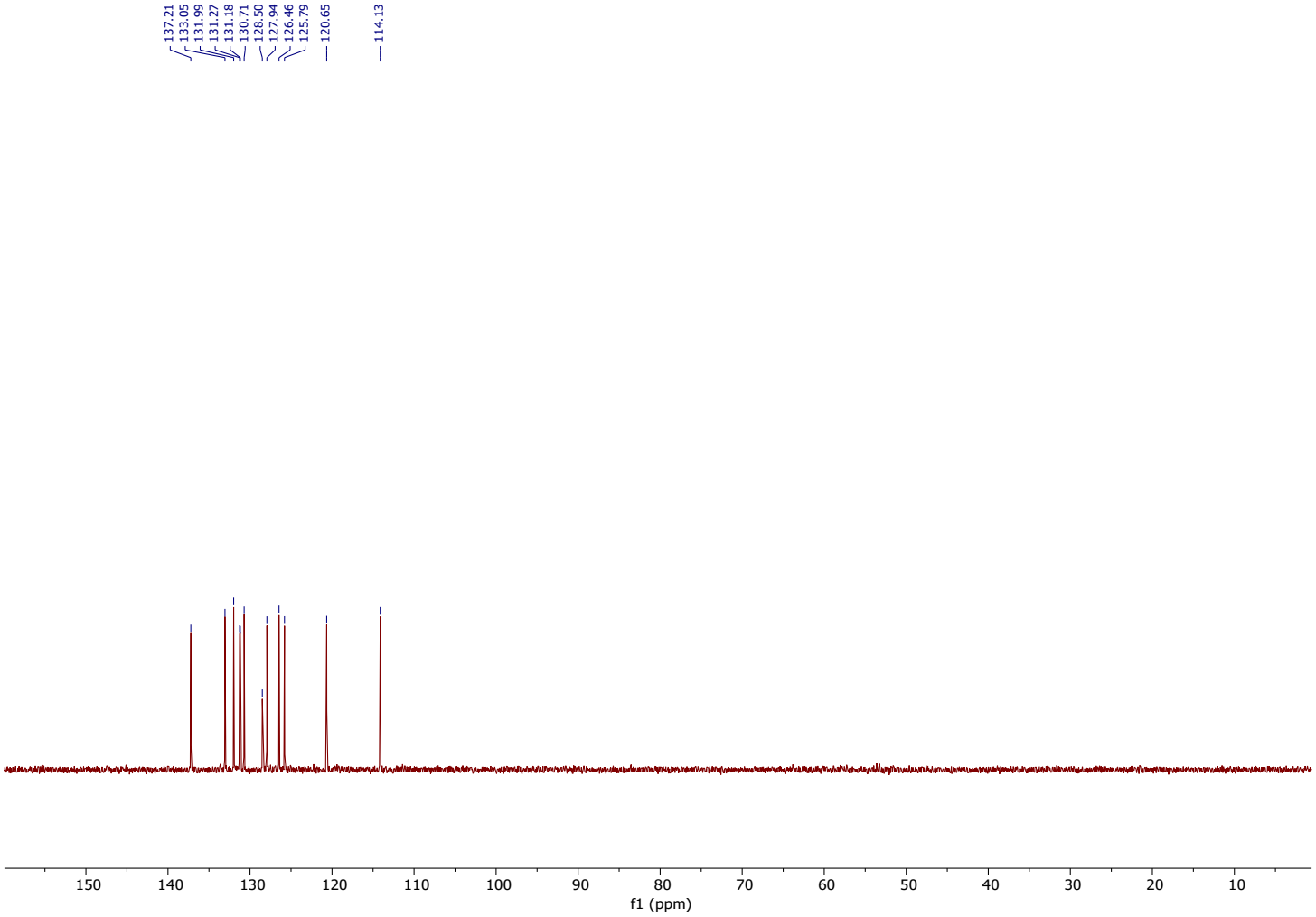

Figure S 22 ***SPA-DBS*** *^{13}C-DEPT135-CD_2Cl_2*

9.4 SIA-DBS – ^1H – CD_2Cl_2

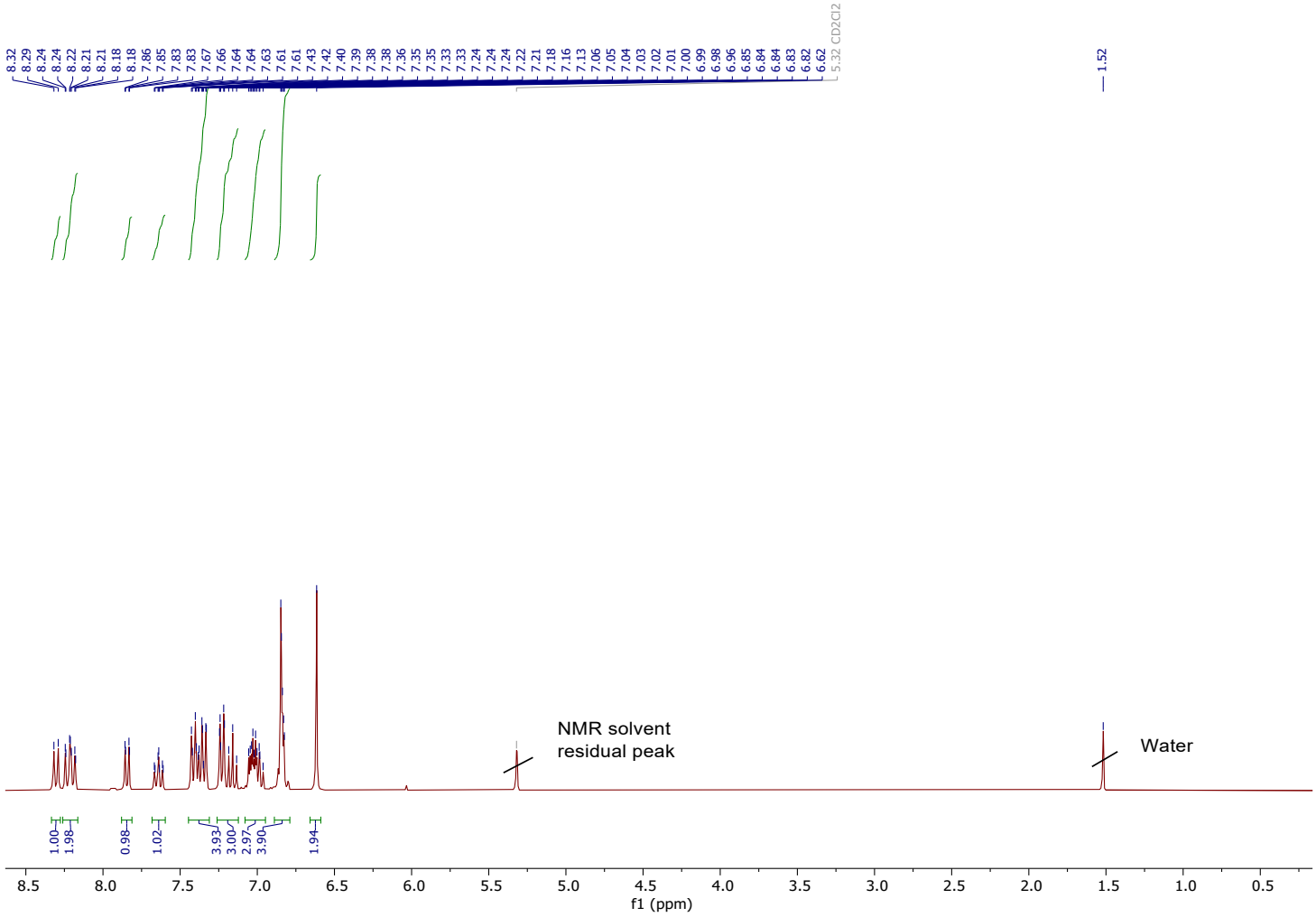

Figure S 23 ***SIA-DBS*** *– ^1H – CD_2Cl_2*

9.5 SIA-DBS – ^{13}C – CD_2Cl_2

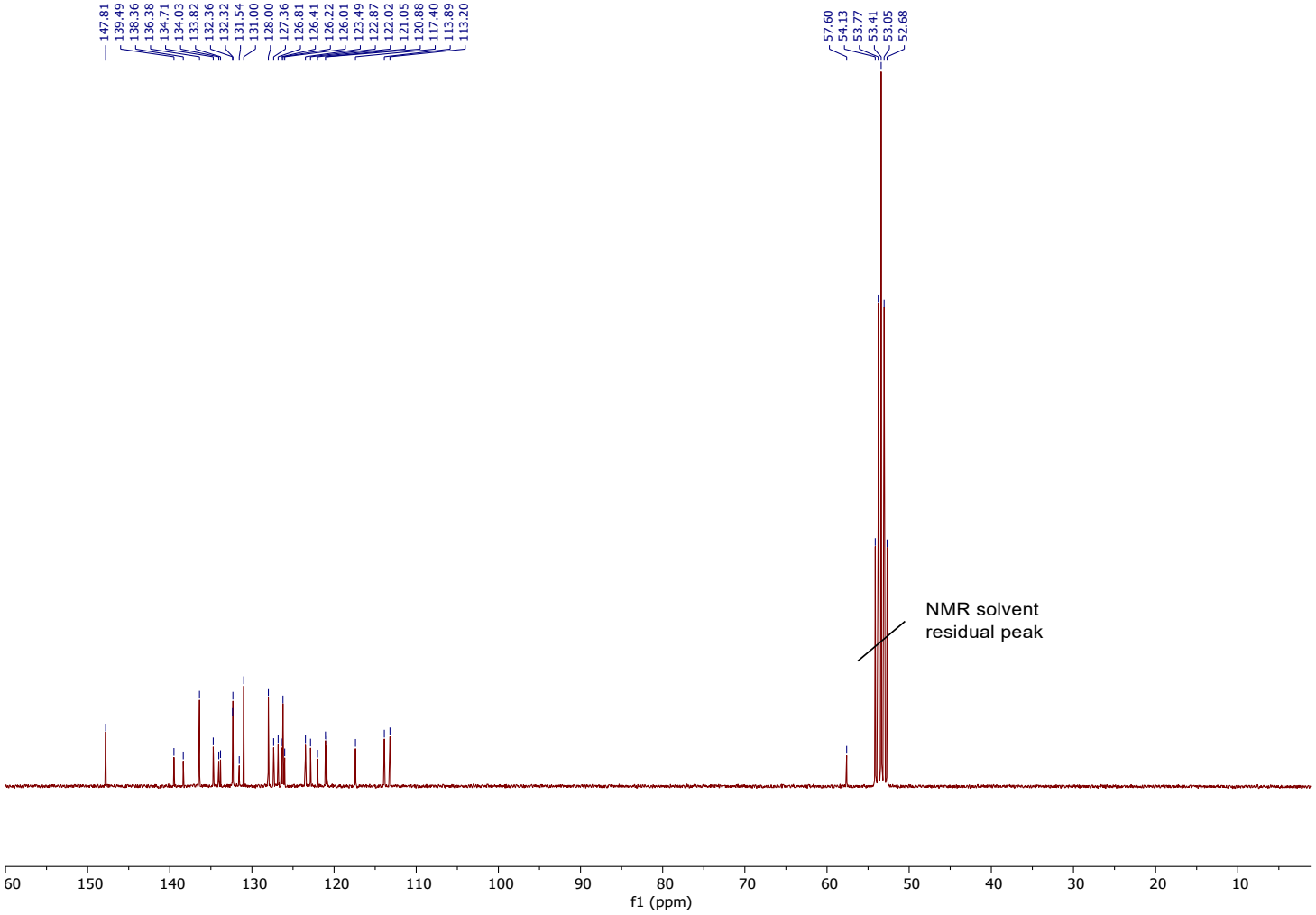

Figure S 24 ***SIA-DBS*** *– ^{13}C – CD_2Cl_2*

9.6 SIA-DBS ^{13}C-DEPT135-CD_2Cl_2

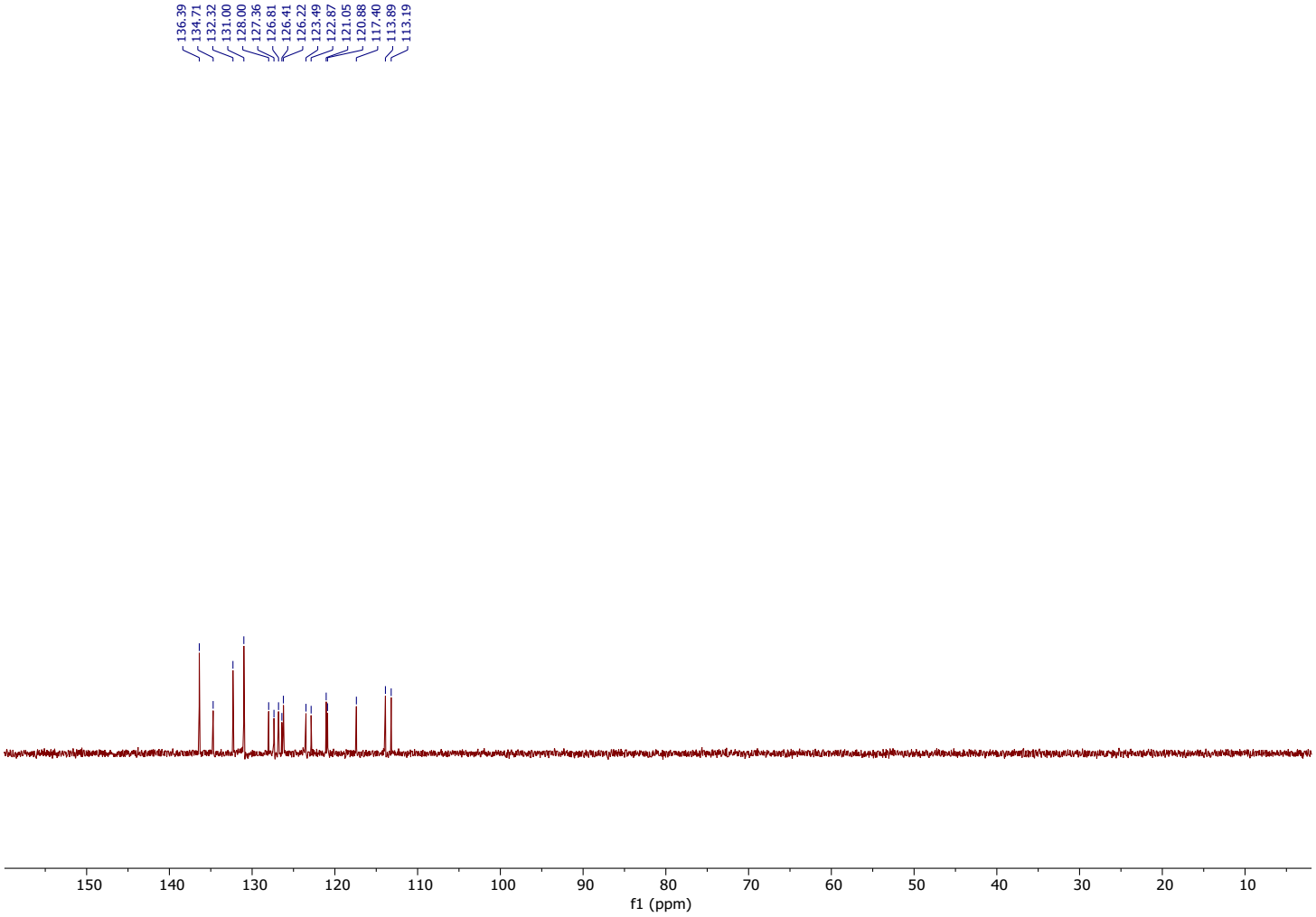

Figure S 25 ***SIA-DBS*** *^{13}C-DEPT135-CD_2Cl_2*

9.7 SQPTZ-DBS – ^1H – CD_2Cl_2

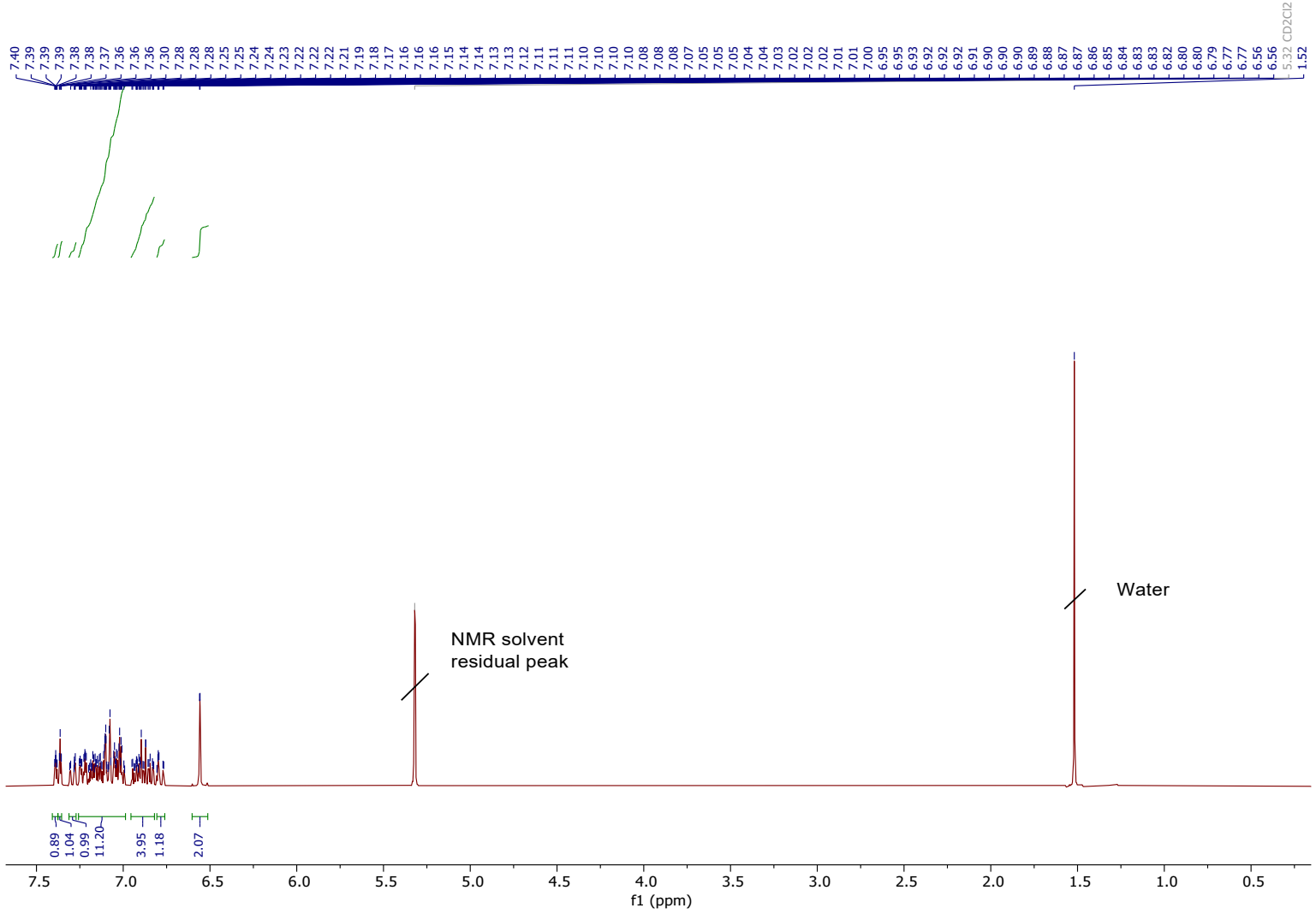

Figure S 26 ***SQPTZ-DBS*** *– ^1H – CD_2Cl_2*

9.8 SQPTZ-DBS – ^{13}C – CD_2Cl_2

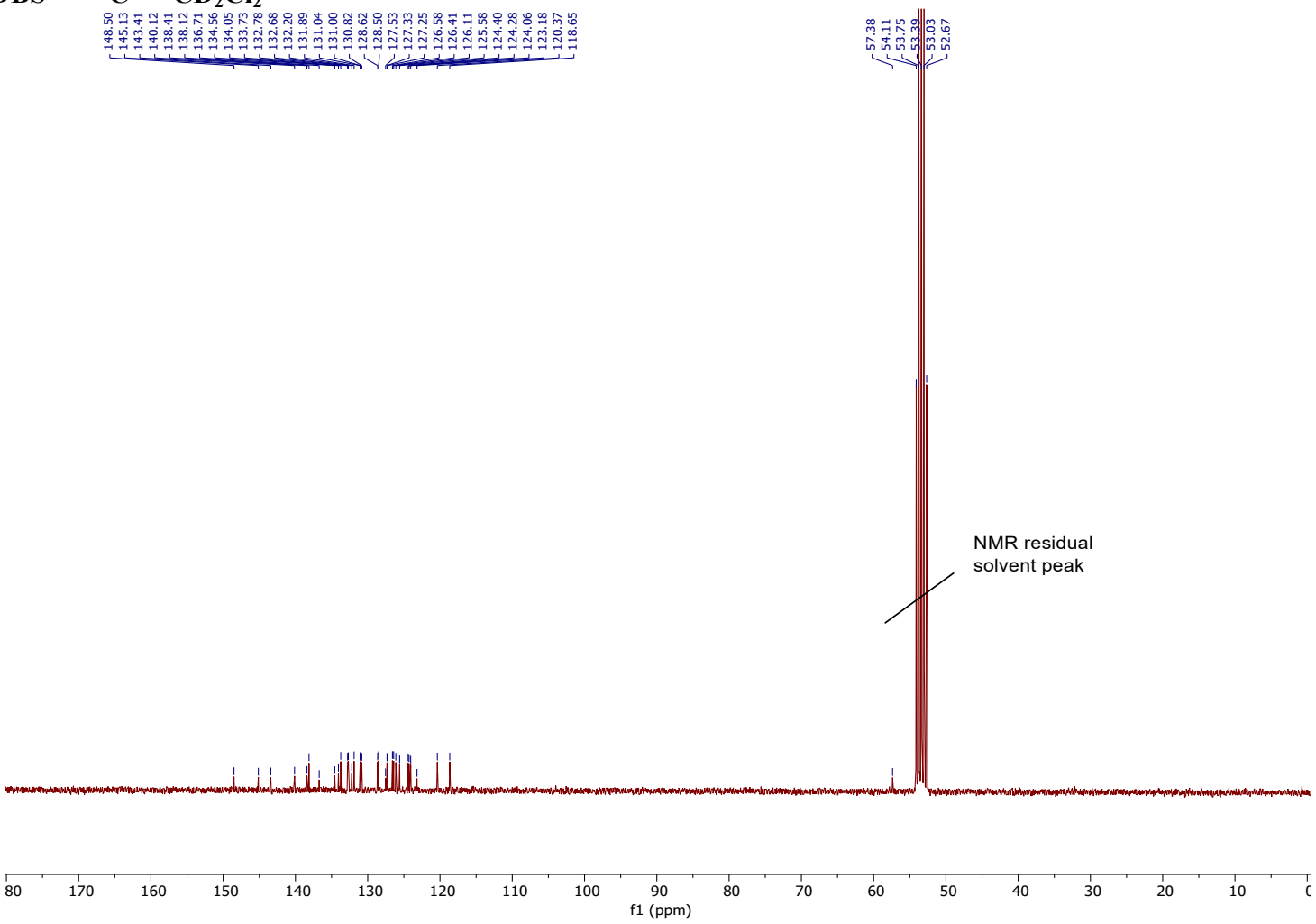

Figure S 27 **SQPTZ-DBS** – ^{13}C – CD_2Cl_2

9.9 SQPTZ-DBS ^{13}C-DEPT135-CD_2Cl_2

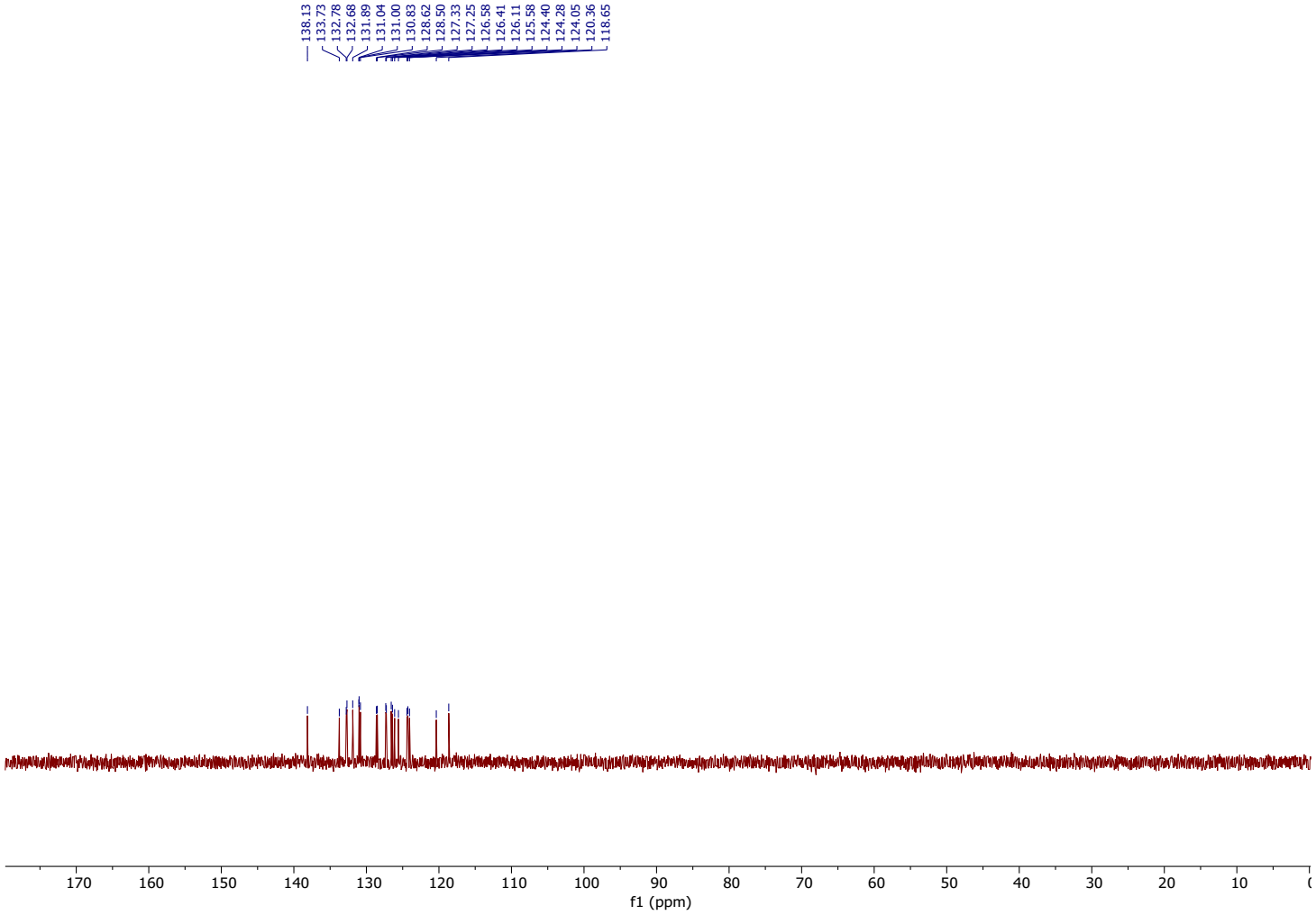

Figure S 28 ***SQPTZ-DBS*** *^{13}C-DEPT135-CD_2Cl_2*

10 Copy of mass spectra

10.1 SPA-DBS

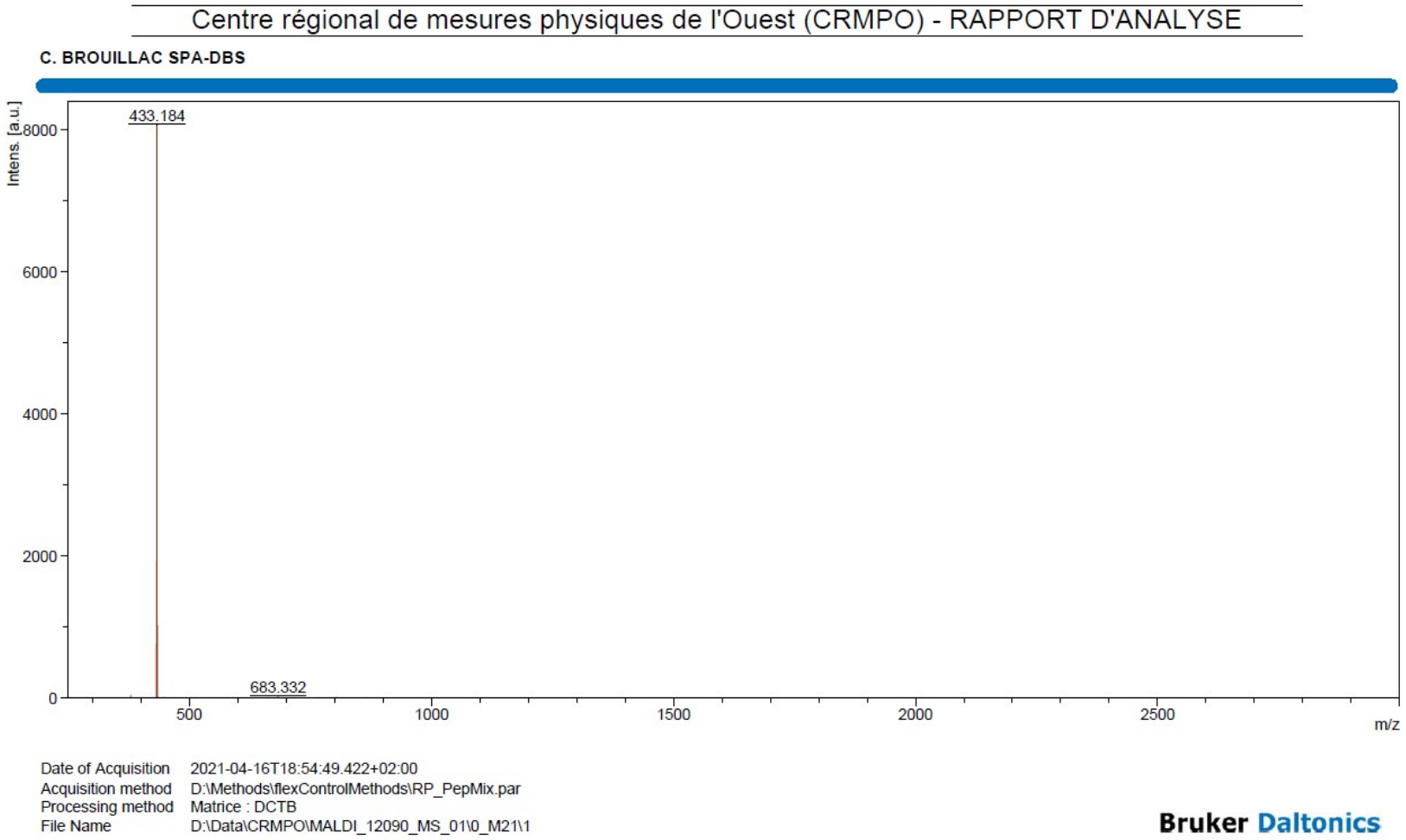

*Figure S 29 HRMS spectrum of **SPA-DBS***

10.2 SIA-DBS

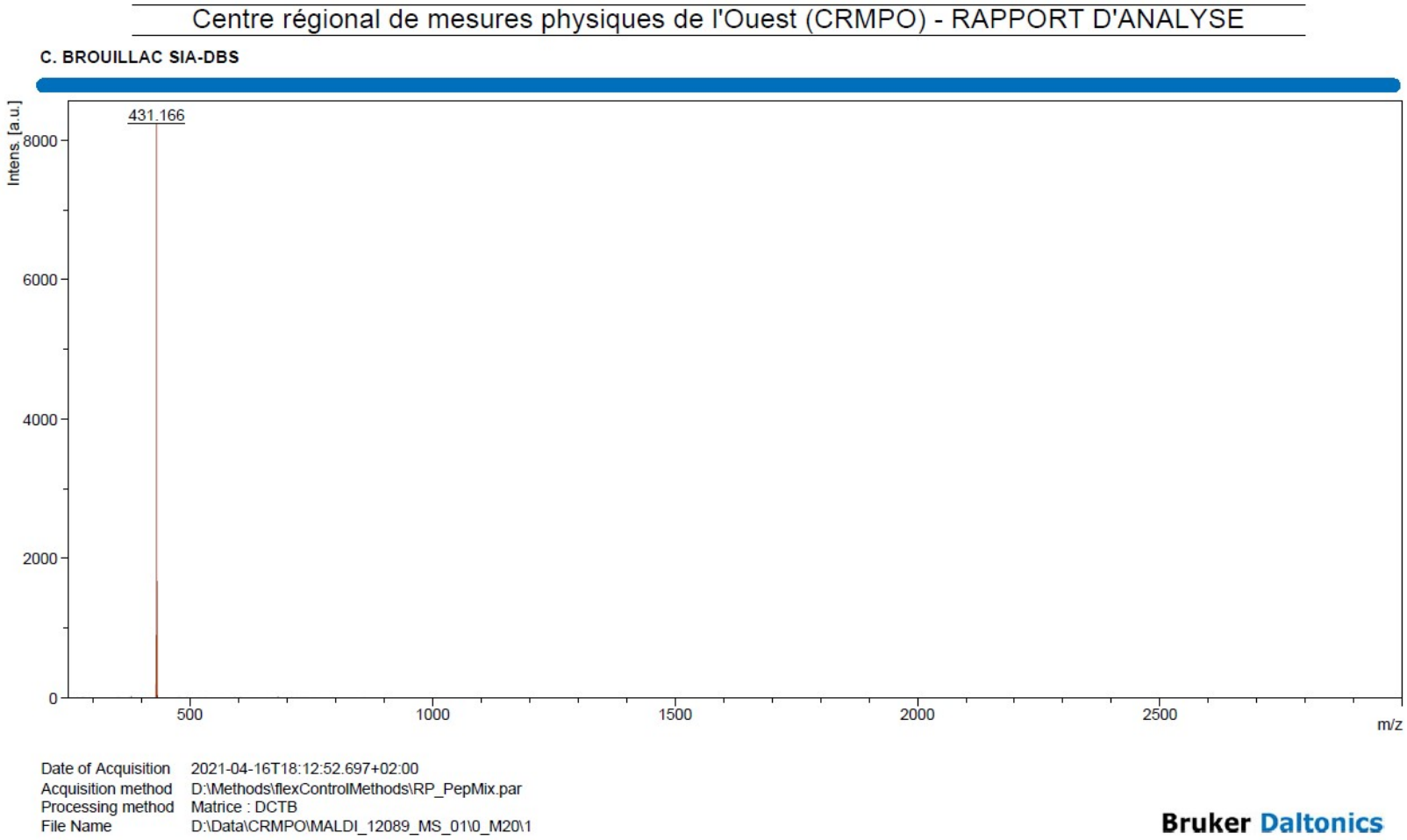

*Figure S 30 HRMS spectrum of **SIA-DBS***

10.3 SQPTZ-DBS

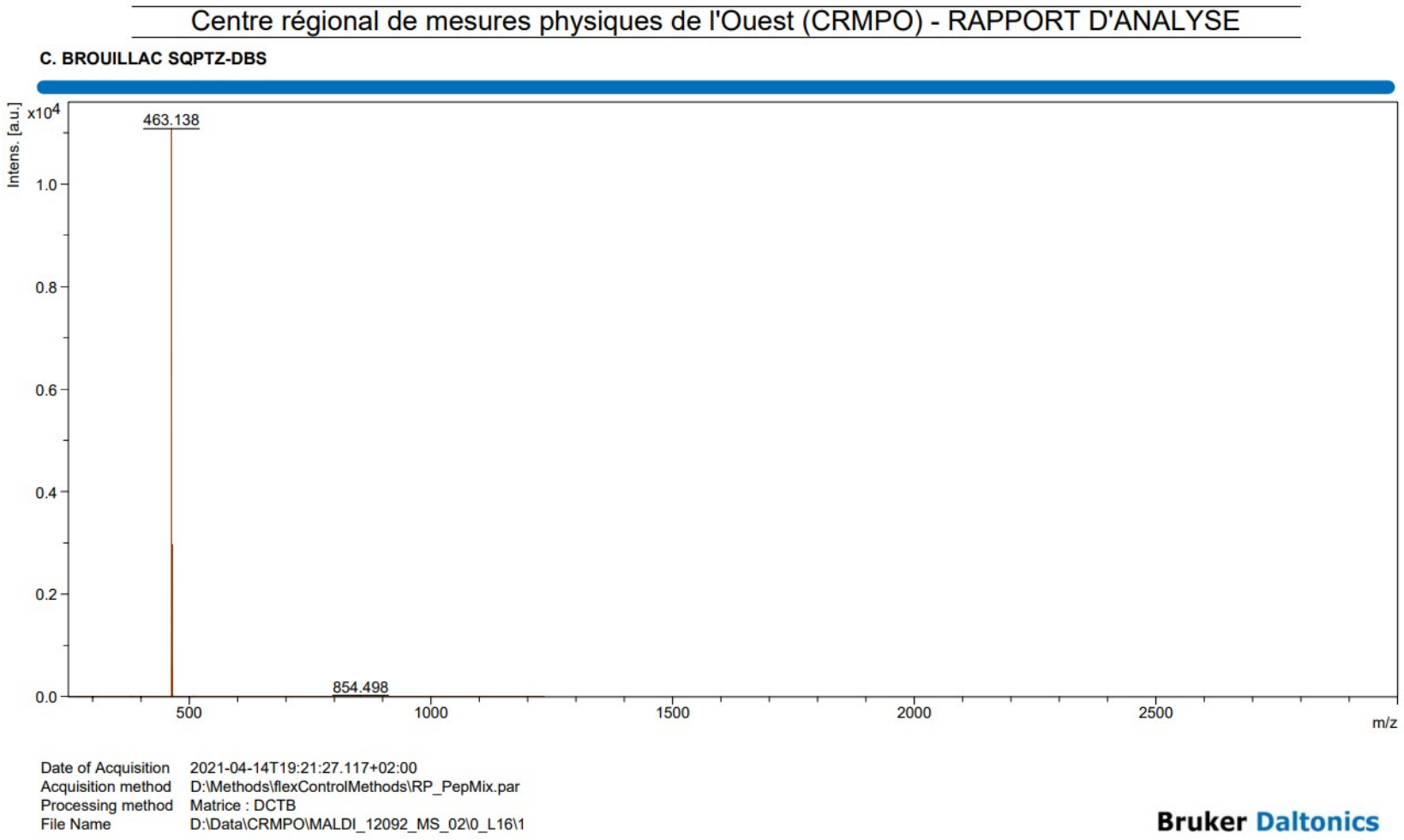

Figure S 31 HRMS spectrum of ***SQPTZ-DBS***

REFERENCES

1. Fulmer, G. R.; Miller, A. J. M.; Sherden, N. H.; Gottlieb, H. E.; Nudelman, A.; Stoltz, B. M.; Bercaw, J. E.; Goldberg, K. I., *Organometallics* 2010, **29**, 2176.
2. Altomare, A.; Cascarano, G.; Giacovazzo, C.; Guagliardi, A.; Burla, M. C.; Polidori, G.; Camalli, M., *J. Appl. Cryst.* 1994, **27**, 435.
3. Sheldrick, G., *Acta Cryst. C* 2015, **71**, 3.
4. Farrugia, L., *J. Appl. Cryst.* 2012, **45**, 849.
5. Lippert, E., *Zeitschrift für Naturforschung A* 1955, **10**, 541.
6. Ooshika, Y., *J. Phys. Soc. Jpn* 1954, **9**, 594.
7. Mataga Noboru ; Kaifu Yozo; Masao, K., *Bull. Chem. Soc. Jpn* 1956, **29**, 465.
8. Kulkarni, A. P.; Tonzola, C. J.; Babel, A.; Jenekhe, S. A., *Chem. Mater.* 2004, **16**, 4556.
9. Kohn, P. H. a. W., *Phys. Rev.* **136**, B864.
10. Calais, J.-L., *Int. J. Quantum Chem.* 1993, **47**, 101.
11. Becke, A. D., *J. Phys. Chem.* 1993, **98**, 1372.
12. Becke, A. D., *J. Phys. Chem.* 1993, **98**, 5648.
13. Becke, A. D., *Phys. Rev. A* 1988, **38**, 3098.
14. Lee C., Y. W. a. R. G. P., *phys. rev. B* 1988, **37**, 785.
15. M. J. Frisch, G. W. T., H. B. Schlegel, G. E. Scuseria, M. A. Robb, J. R. Cheeseman, G. Scalmani, V. Barone, B. Mennucci, G. A. Petersson, H. Nakatsuji, M. Caricato, X. Li, H. P. Hratchian, A. F. Izmaylov, J. Bloino, G. Zheng, J. L. Sonnenberg, M. Hada, M. Ehara, K. Toyota, R. Fukuda, J. Hasegawa, M. Ishida, T. Nakajima, Y. Honda, O. Kitao, H. Nakai, T. Vreven, J. A. J. Montgomery, J. E. Peralta, F. Ogliaro, M. Bearpark, J. J. Heyd, E. Brothers, K. N. Kudin, V. N. Staroverov, T. Keith, R. Kobayashi, J. Normand, K. Raghavachari, A. Rendell, J. C. Burant, S. S. Iyengar, J. Tomasi, M. Cossi, N. Rega, J. M. Millam, M. Klene, J. E. Knox, J. B. Cross, V. Bakken, C. Adamo, J. Jaramillo, R. Gomperts, R. E. Stratmann, O. Yazyev, A. J. Austin, R. Cammi, C. Pomelli, J. W. Ochterski, R. L. Martin, K. Morokuma, V. G. Zakrzewski, G. A. Voth, P. Salvador, J. J. Dannenberg, S. Dapprich, A. D. Daniels, O. Farkas, J. B. Foresman, J. V. Ortiz, J. Cioslowski, D. J. Fox, 2010, Gaussian 09.
16. Lucas, F.; Tondelier, D.; Geffroy, B.; Heiser, T.; Ibraikulov, O. A.; Quinton, C.; Brouillac, C.; Leclerc, N.; Rault-Berthelot, J.; Poriel, C., *Mater, Chem, Front* 2021, **5**, 8066.
17. Li, B.; Gong, Y.; Wang, L.; Lin, H.; Li, Q.; Guo, F.; Li, Z.; Peng, Q.; Shuai, Z.; Zhao, L.; Zhang, Y., *J. Phys. Chem. Lett.* 2019, **10**, 7141.
18. Chien-Tien Chen; Yi Wei, J.-S. L.; Murthy V. R. K. Moturu; Wei-San Chao; Yu-Tai Tao; Chien, C.-H., *J. Am. Chem. Soc.* 2006, **128**, 10992.
19. Lucas, F.; Ibraikulov, O. A.; Quinton, C.; Sicard, L.; Heiser, T.; Tondelier, D.; Geffroy, B.; Leclerc, N.; Rault‐Berthelot, J.; Poriel, C., *Adv. Opt. Mater.* 2019, **8**, 1901225.
20. Thiery, S.; Tondelier, D.; Geffroy, B.; Jeannin, O.; Rault-Berthelot, J.; Poriel, C., *Chem. Eur. J* 2016, **22**, 10136.
21. Zou, S. N.; Chen, X.; Yang, S. Y.; Kumar, S.; Qu, Y. K.; Yu, Y. J.; Fung, M. K.; Jiang, Z. Q.; Liao, L. S., *Adv. Opt. Mater.* 2020, **8**, 2001074.